Characterization of *Saccharomyces cerevisiae* tRNA nucleotidyltransferase variants

Prit-Kamal Singh Sandhu

A Thesis

in

The Department

of

Chemistry and Biochemistry

Presented in Partial Fulfillment of the Requirements

for the Degree of Master of Science (Chemistry) at

Concordia University

Montreal, Quebec, Canada

September 2014

CONCORDIA UNIVERSITY

School of Graduate Studies

This is to certify that the thesis prepared

By: Prit-Kamal Singh Sandhu

Entitled: Characterization of *Saccharomyces cerevisiae* tRNA nucleotidyltransferase variants

and submitted in partial fulfillment of the requirements for the degree of

Master of Science (Chemistry)

complies with the regulations of the University and meets the accepted standards with respect to originality and quality.

Signed by the final Examining Committee:

Dr. George Denes_____ Chair

Dr. Peter Pawelek_____ Examiner

Dr. Joanne Turnbull_____ Examiner

Dr. Paul Joyce_____ Supervisor

Approved by _____Dr. Heidi Muchall_____

Chair of Department or Graduate Program Director

Date: September 15th 2014 ____André Roy_____

Dean of Faculty

Abstract

Yeast cells exhibit a temperature-sensitive phenotype at 37°C due to an ATP(CTP): tRNA nucleotidyltransferase variant containing a glutamate to phenylalanine substitution at position 189. This amino acid alteration in conserved motif C results in weakened thermal stability and reduced enzyme activity in the tRNA nucleotidyltransferase. When the arginine at position 64 of this enzyme is changed to tryptophan, enzyme activity is increased and the temperature-sensitive phenotype is suppressed such that the yeast can grow at the restrictive temperature. This suppressor mutation is found associated with the highly conserved motif A which plays a crucial role in catalysis. Here the roles of glutamate 189 and arginine 64 in tRNA nucleotidyltransferase activity are explored. The data presented here show that the decrease in enzyme activity in the enzyme bearing the glutamate to phenylalanine substitution at position 189 results from an approximately 70-fold decrease in catalytic activity (k_{cat}) and a less than 2-fold change in apparent tRNA binding (K_M). Moreover, they show that the subsequent arginine to tryptophan substitution at position 64 results in an approximate 6-fold increase in enzyme activity as compared to the glutamate to phenylalanine substitution variant with no apparent change in K_M. Interestingly, the arginine to tryptophan substitution alone shows no major change to either apparent k_{cat} or K_M as compared to the native enzyme. Based on these observations, molecular modeling suggests that the glutamate to phenylalanine substitution in motif C affects catalysis by altering the organization of catalytic residues in the head and neck regions of the protein. Substitution of glutamate at position 189 by a larger amino acid produces steric repulsion that disturbs the precise positioning of motif A and B residues leading to a reduced k_{cat}. These data also suggest that the organization of the head and neck regions of the protein do not play a major role in tRNA binding. Finally, the suppressor mutation resulting in the change of arginine 64 to tryptophan allows the catalytic residues of motifs A and B to be shielded from steric hindrance leading to the measured increase in k_{cat} that restores viability at the restrictive temperature.

Acknowledgements

I would like to thank my supervisor, Dr. Paul Joyce, for giving me this project, his constructive criticism and his editorial prowess. Then, there is also Pam Hanic-Joyce for her tremendous help in the laboratory mostly with molecular biology related materials and methods. Also, Matthew Leibovitch was an essential colleague with his operational expertise and quick thinking.

List of Figures

List of Tables

List of Abbreviations

APS: Ammonium persulfate

ATP: Adenosine triphosphate

CTP: Cytidine triphosphate

CCA: cytidine-cytidine-adenosine

dH_2O: distilled water

GST: Glutathione-S-transferase

GTP: Guanosine triphosphate

IPTG: Isopropyl-β-D-Thiogalactopyranoside

K_M: Michaelis-Menten constant

k_{cat}: Turnover number

kDa: Kilodaltons

NTP: Nucleotide triphosphate

O.D.: Optical density

PBS: Phosphate Buffered Saline

SDS-PAGE: Sodium Dodecyl Sulfate-Polyacrylamide Gel Electrophoresis

TBE: Tris Borate EDTA

TEMED: Tetramethylethylenediamine

T_m: Melting temperature

tRNA: transfer Ribonucleic Acid

YT: Yeast tryptone

TABLE OF CONTENTS

1.0 INTRODUCTION

1.1 Transfer RNAs

Transfer RNAs (tRNAs) are important adapter molecules in cells. Each tRNA carries an amino acid which will be incorporated into the growing polypeptide chain at the ribosome as defined by the appropriate mRNA codon. The biosynthesis of a functional tRNA requires a number of steps including, transcription of the gene, 5' and 3' processing of the primary transcript, removal of any introns, specific sugar and base modifications and, if necessary, addition of the 3'terminal cytidine, cytidine, and adenosine residues (Deutscher, 1973). This terminal cytidine, cytidine, adenosine (CCA) sequence, positions 74, 75 and 76 in the standardized tRNA structure (Fig. 1-1), is essential for amino acid acceptance and peptide bond formation (Deutscher, 1973). While some organisms, *e.g., Escherichia coli*, encode this sequence in their tRNA genes, many others must have this CCA sequence added post-transcriptionally (Sprinzl and Cramer, 1979).

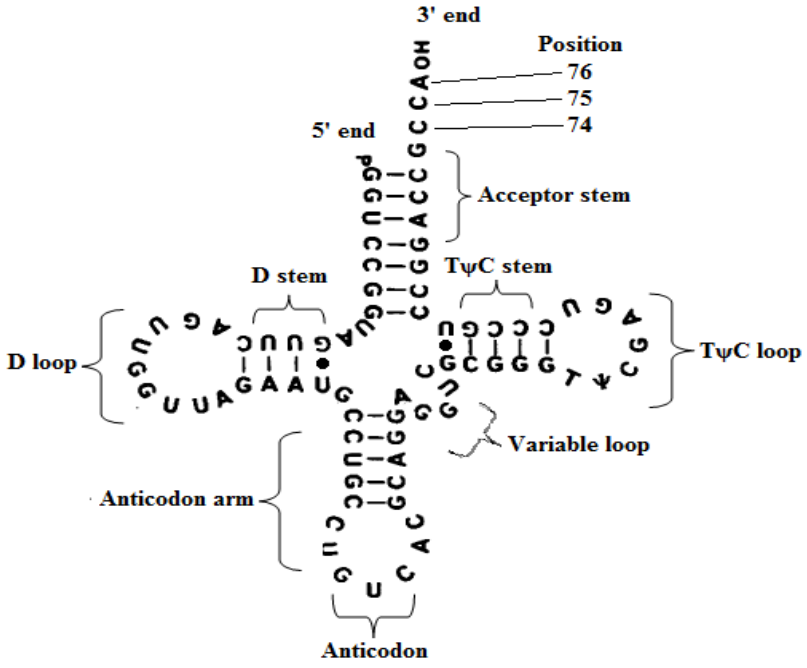

Figure 1-1. Classical secondary structure of transfer RNA. This is the structure of the $tRNA^{Asp}$ from *Bacillus subtilis.* Dashes (—) represent standard Watson-Crick base pairs while dots (●) indicate non-standard base pairs. This figure was acquired and modified from Yamada *et al*. (1983).

1.2 tRNA nucleotidyltransferase

The enzyme responsible for the addition of the CCA sequence is ATP(CTP):tRNA nucleotidyltransferase (EC 2.7.7.25). In eukaryotes this enzyme is required in all of the translationally-active compartments of the cell (*i.e.*, cytosol, mitochondrion and in plants, plastid) where it ensures that tRNAs are made with intact CCA sequences. In the cytosol, in addition to adding the CCA sequence to tRNAs that are transcribed lacking this sequence, this enzyme also may play a role in repairing damaged CCA ends (Lizano *et al*., 2008). It likely has a similar repair function in *E. coli* (where the primary transcripts contain the CCA sequence) as removing the gene coding for this enzyme is not lethal but results in a reduced growth rate (Zhu and Deutscher, 1987). Cytosolic tRNA nucleotidyltransferase also may have a role in quality control, for example, recently tRNA nucleotidyltransferase has been shown to add a CCACCA to the 3`-termini of certain classes of tRNAs to direct them to the rapid tRNA decay pathway (Wilusz *et al*., 2011). Similarly, nuclear CCA addition is thought to provide a quality control step to ensure that only mature tRNAs are released from the nucleus to the cytosol to participate in protein synthesis (Zasloff *et al.,* 1982, Zasloff, 1983). The nuclear localization of tRNA nucleotidyltransferase also may reflect a role in nuclear/cytosolic shuttling of tRNAs (Feng and Hopper, 2002). Nucleocytoplasmic shuttling of tRNAs has been implicated in the regulation of processes as diverse as protein synthesis (Chu and Hopper, 2013), the cell cycle (Ghavidel *et al*., 2007), and nutrient availability (Whitney *et al*., 2007). Given that tRNAs may undergo retrograde transport into the nucleus under specific stress conditions (Murthi *et al*., 2010, Czech *et al*., 2013) and that tRNA nucleotidyltransferase functions both in the cytosol and the nucleus, tRNA nucleotidyltransferase localization also may be regulated in this context. Intriguingly, in the eukaryotes studied to date (*e.g*., Chen *et al*., 1992, Shanmugam *et al*., 1996, Deng *et al*., 2000, Reichert *et al*., 2001, Nagaike *et al*., 2001, Schmidt von Braun *et al*., 2007) a single nuclear gene is responsible for generating the various forms of tRNA nucleotidyltransferase found in the cell. While considerable effort has gone into studying the regulation and control of sorting of this protein these studies are beyond the scope of this thesis. Instead this report will concentrate on the structure and function of this interesting enzyme.

1.3 The nucleotidyltransferase superfamily

1.3.1 polymerase β family

The tRNA nucleotidyltransferase enzyme is a polymerase belonging to the polymerase β family of enzymes (Holm and Sander, 1996, Aravind and Koonin, 1999). The enzymes in this family catalyze a large number of different reactions but all are involved in nucleotide transfer (Holm and Sander, 1996). The consensus sequence hG[GS]x(9,13)Dh[DE]h (where h is a conserved histidine residue, G, S, D and E are invariant glycine, serine, aspartate and glutamate residues, respectively, and x is any amino acid) is common to all enzymes of this family (Aravind and Koonin, 1999). It is a signature catalytic motif that is found in the head domain of all enzymes of this family.

The polymerase β family of enzymes has been divided into two classes based on sequence similarity (Yue *et al*., 1996). Class I enzymes include terminal nucleotidyltransferases (TdT), antibiotic nucleotidyltransferases, protein nucleotidyltransferases, 2'-5' oligo(A) synthetases, Trf4-like polyA polymerases, archael tRNA nucleotidyltransferases and many others (Yue *et al*., 1996). Class II enzymes consist of a smaller group which is composed of bacterial and eukaryotic tRNA nucleotidyltransferases, and bacterial poly(A) polymerases (Yue *et al*., 1996). Recent studies have shown that while in many organisms CCA addition is carried out by a single enzyme, there are other organisms (*e.g*., *Aquifex aeolicus*, *Deinococcus radiodurans*; *Synechocystis* sp., *Bacillus halodurans*) that have separate but related CC- and A-adding enzymes that are required for complete CCA addition (reviewed in Neuenfeldt *et al*., 2008). It is likely that all of these enzymes evolved from minimal nucleotidyltransferases which were themselves descendants of an ancient RNA world telomerase (Betat *et al*., 2010).

1.3.2 tRNA nucleotidyltransferases

Class I tRNA nucleotidyltransferases show a structure defined by four domains (N-terminal, central, C-terminal and tail) arranged in an overall U shape (Figure 1-2). The N-terminal domain contains a five-stranded β-sheet and two α-helices as well as three catalytic

residues (Glu59, Asp61, and Asp110) which are found on the β-sheet. These three carboxylates are found close together in space and coordinate the catalytically important Mg^{++} ion. The active site pocket of a Class I enzyme can be used for both C and A addition because the folding of the 3'-terminus of the tRNA in the pocket as well as the shape of the pocket itself change after nucleotide addition such that the terminus of the tRNA is oriented correctly at the active site for C addition at positions 74 and 75 and then A addition at position 76 (reviewed in Tomita and Yamashita, 2014). Taken together these data suggest that the template of the Class I CCA-adding enzyme is neither the protein nor the RNA, but the RNA–protein complex (Tomita and Yamashita, 2014).

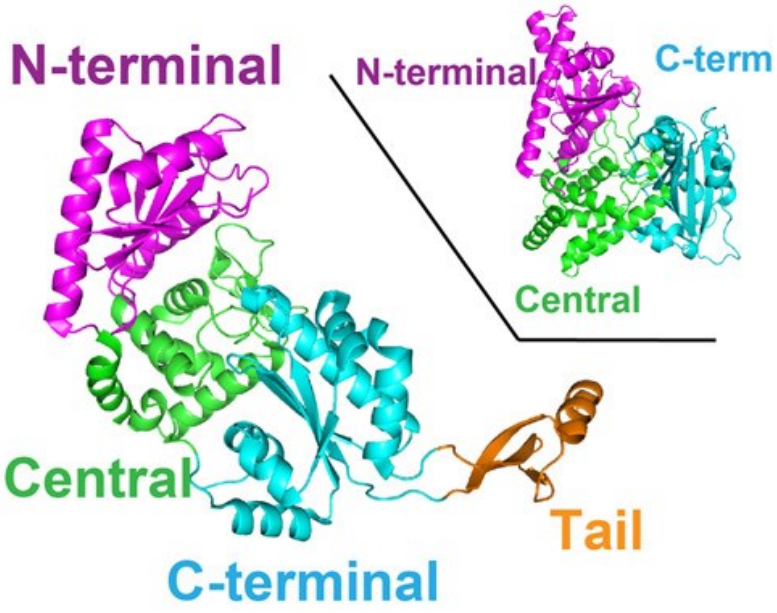

Figure 1-2. Structure of Class I tRNA nucleotidyltransferase from *Archaeoglobus fulgidus*. This figure was acquired and modified from Tomita and Yamashita (2014).

In contrast, crystallographic studies (Li *et al*., 2002, Augustin *et al*., 2003, Tomita *et al*., 2004, Toh *et al*., 2009) have shown that the Class II CCA-adding enzyme takes on a seahorse-like shape composed of head, neck, body and tail domains (Fig. 1-3, Xiong *et al*., 2002). Again as in class I enzymes, the only β-sheet is found within the amino-terminal head domain and contains the three conserved catalytic carboxylate residues involved in catalysis. The rest of the protein`s structure is composed of alpha-helical elements (reviewed in Betat *et al*., 2010). The

important nucleobase-interacting residues (defined as an aspartate and an arginine) are found in the neck domain while the body and tail are thought to recognize the acceptor and TΨC regions of the tRNA (reviewed in Tomita and Yamashita, 2014). The mechanism for CCA addition by Class II enzymes differs from that of Class I enzymes in that the protein itself provides the template for nucleotide addition instead of the RNA-protein complex providing the template as in Class I enzymes (reviewed in Tomita and Yamashita, 2014).

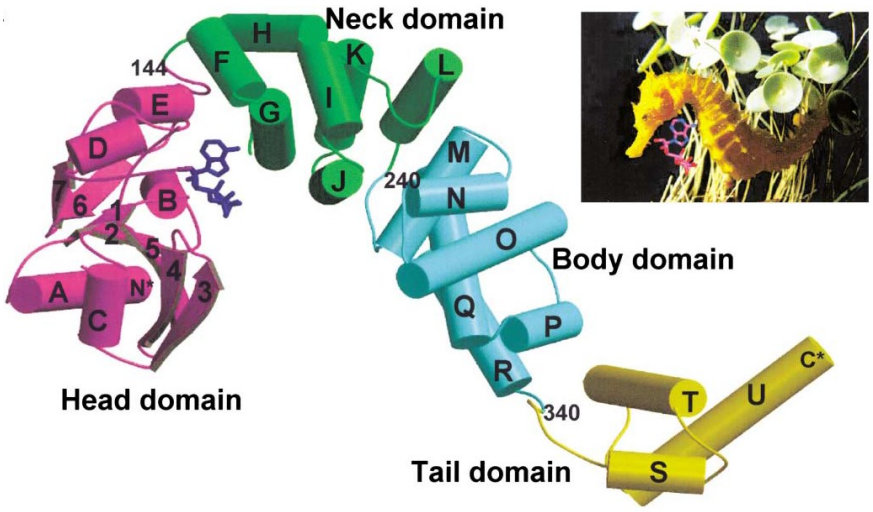

Figure 1-3. Model of Crystal Structure of *Bacillus stearothermophilus* tRNA nucleotidyltransferase. The crystal structure of *Bacillus stearothermophilus* tRNA nucleotidyltransferase is shown here complexed with a tRNA mimic. Image taken from Li *et al*. (2002).

1.3.3 Conserved motifs in Class II tRNA nucleotidyltransferases

Based on amino acid alignments five conserved motifs (A-E) have been identified in Class II tRNA nucleotidyltransferases (Fig. 1-4, Li *et al*. 2002). The functions associated with each of these motifs will be discussed below.

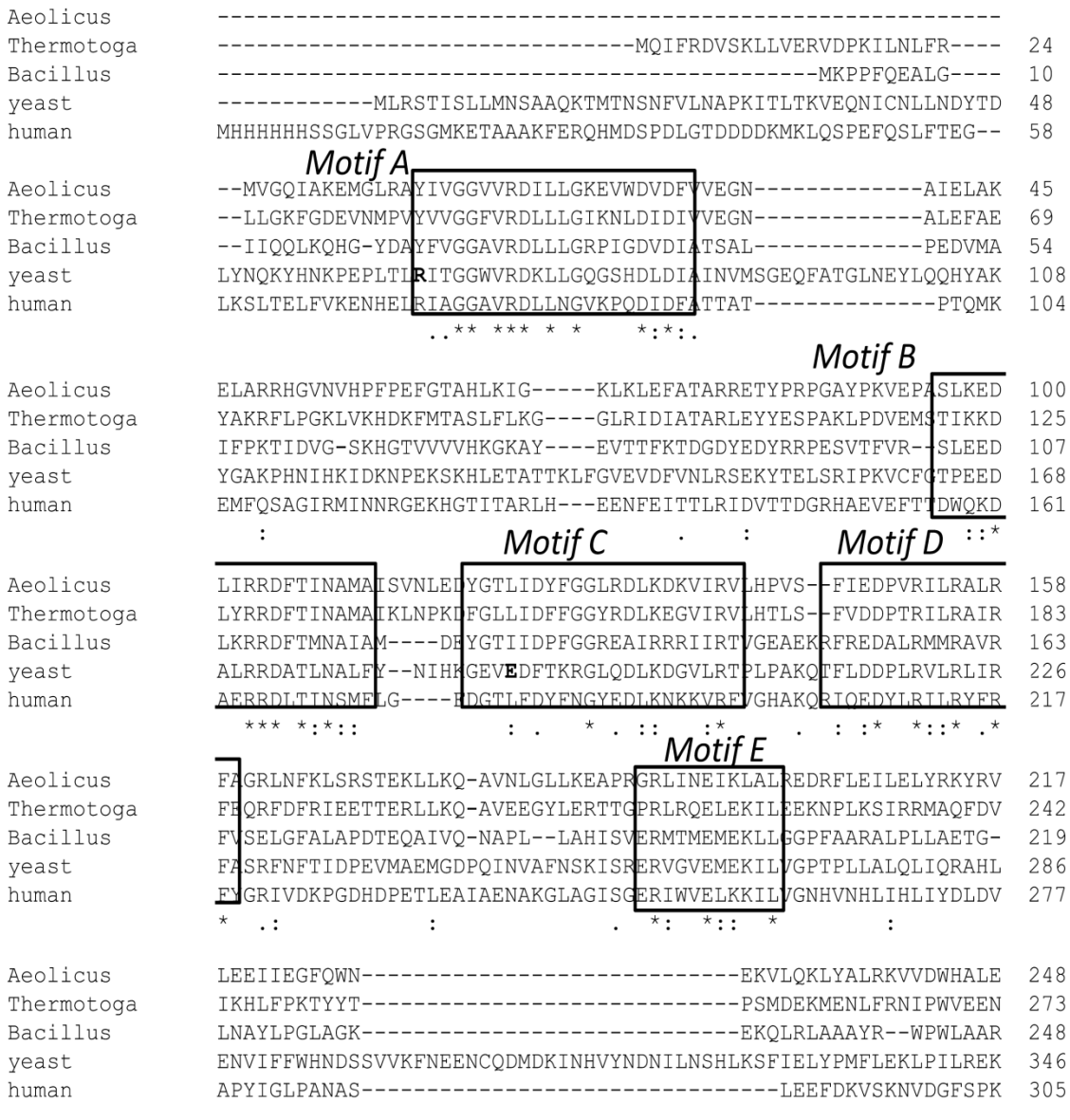

Figure 1-4 ClustalW (Larkin *et al*., 2007) alignment of the head and neck regions of *Saccharomyces cerevisiae*, *Aquifex aeolicus*, *Thermotoga maritima*, *Bacillus stearothermophilus* and human tRNA nucleotidyltransferases. Motifs A-E first identified in the *B. stearothermophilus* enzyme (Li *et al*., 2002) are boxed and labelled. Residues R64 and E189 in the *S. cerevisiae* enzyme (the amino acids of importance in this work) are in bold. (*) amino acid identity, (:) strongly conserved amino acid, (.) weakly conserved amino acid. Taken from Goring *et al*. (2013).

1.3.3.1 Motif A

Motif A is found in the head domain. It contains a highly conserved GGxVRD sequence and an absolutely conserved DxD sequence (Fig. 1-4). The three carboxylate aspartate residues coordinate the two metal ions that facilitate the polymerization reaction and the binding of the triphosphate moiety of incoming NTPs (Fig. 1-5, Li *et al*., 2002).

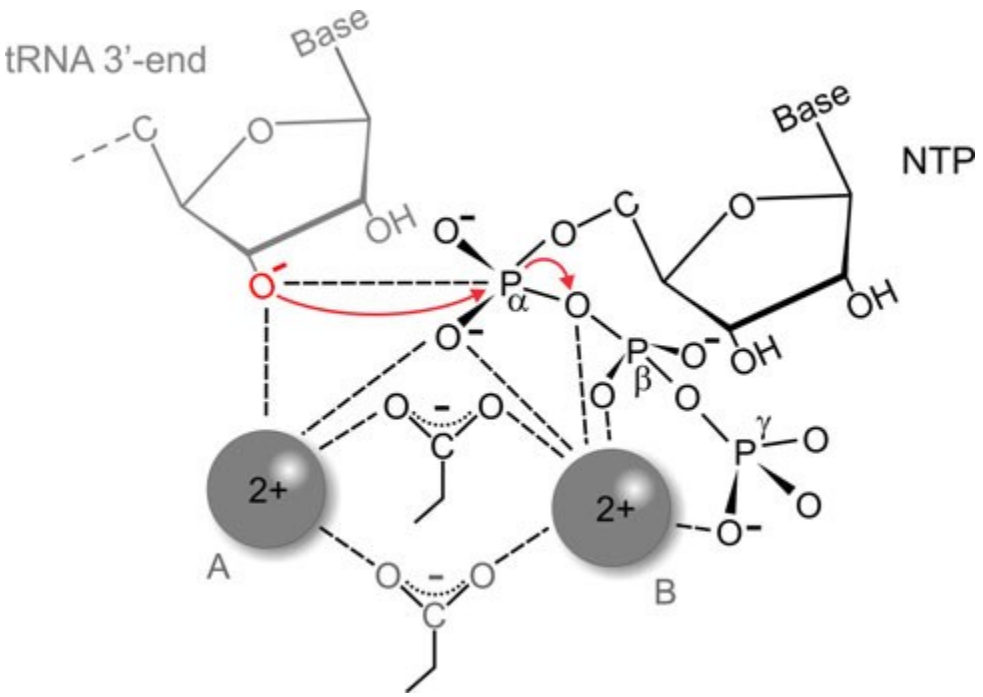

Figure 1-5. Reaction Mechanism of DxD NTP addition. Two aspartates coordinate two magnesium ions to ready the alpha phosphate of the incoming NTP for nucleophilic attack from 3'-O^- of the tRNA primer. Image taken from Betat *et al*. (2010).

1.3.3.2 Motif B

Motif B, also found in the head region, contains the highly conserved RRD sequence (Fig. 1-4) which allows recognition of the nucleotide triphosphate's ribose moiety and specifically its 2'-OH thus discriminating against deoxyribonucleotides as shown by site-directed mutagenesis which converted a CCA-adding enzyme into a dCdCdA-adding enzyme (Cho *et al*., 2007).

1.3.3.3 Motif D

Motif D, containing the highly conserved (E/D)DxxR sequence, is found in the neck domain and forms the basis for nucleotide binding with Watson-Crick-like hydrogen bonding between residues of the protein and the cytosine and adenine base moieties of the bound nucleotide triphosphates (Li *et al*., 2002). More specifically, the conserved arginine residue forms two hydrogen bonds with N3 and O2 of the incoming CTP while the aspartate forms one hydrogen bond with the 4-amino group of the base (Fig. 1-6). After CC addition, the active site undergoes a subtle reorganization such that its specificity has changed from CTP binding to ATP binding (Li *et al*., 2002). The glutamate and arginine residues now are involved in ATP recognition, The aspartate forms h-bond with the 6-amino group while the arginine binds the N1 of the ATP (Fig. 1-6). The binding pocket has greater specificity for CTP and ATP than for GTP and UTP due to an incompatible hydrogen bonding pattern with the latter two nucleotides. The importance of these residues in nucleotide addition was shown in experiments where by reversing the polarity of hydrogen bonds between the nucleobases and the protein template, a CCA-adding was transformed into a (U,G)-adding enzyme that incorporate UTP and GTP instead of CTP and ATP (Cho *et al*., 2007).

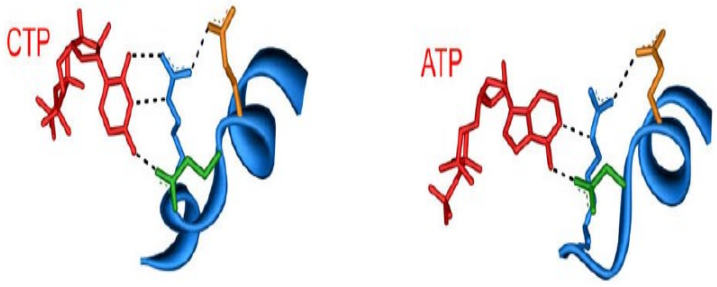

Figure 1-6. Binding of nucleotides by a Class II tRNA nucleotidyltransferase. The crystal structure of a Class II tRNA nucleotidyltransferase is shown here complexed with CTP and ATP. Red is for the respective nucleotide, blue is the arginine that hydrogen bonds with the base, orange is a glutamate (or sometimes aspartate) that helps to orient the arginine and green is for an aspartate that forms an additional hydrogen bond with the base. Image taken from Vortler *et al*. (2010).

1.3.3.4 Flexible loop near the catalytic core

Interestingly, in the context of the specificity of CTP addition versus ATP addition, there is a flexible loop between motifs A and B (Fig. 1-7) and extending between the head and neck domains that appears to play a role in ATP addition but not in CTP addition (Tomita *et al*., 2004; Neuenfeldt *et al*., 2008; Toh *et al*., 2009). This loop likely interacts with the 3'-end of the growing tRNA (Toh *et al*., 2009), recognizes the CC-sequence and fixes the conformation of the catalytically important aspartate and arginine residues to define recognition of ATP. In tRNA nucleotidyltransferases which add only the CC sequence, *e.g*., in *Aquifex aeolicus*, *Deinococcus radiodurans*, *Bacillus halodurans*, and *Synechocystis* sp. this loop is much shorter (reviewed in Neuenfeldt *et al*., 2008).

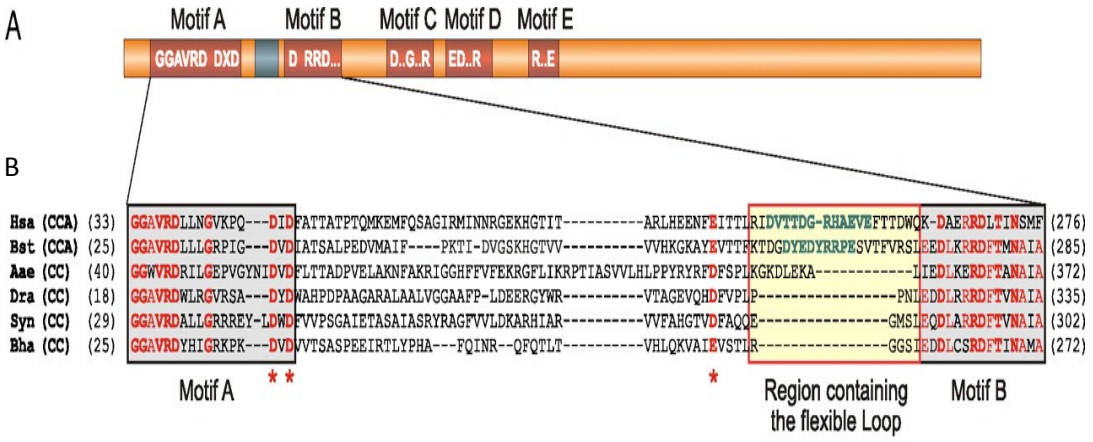

Figure 1-7 Alignment of CC-adding enzymes with CCA-adding enzymes of known crystal structures to show flexible loop region. Hsa, *H. sapiens*; Bst, *Bacillus stearothermophilus*; Aae, *Aquifex aeolicus*; Dra, *Deinococcus radiodurans*; Syn, *Synechocystis* sp.; Bha, *Bacillus halodurans*. Conserved amino acids are shown in panel A and the region between motifs A and B is expanded in panel B. Image taken from Neuenfeldt *et al*. (2008).

1.3.3.5 Motif E

Motif E (Fig. 1-4) may play a number of roles in enzyme activity. Site-directed mutagenesis in helix J found in motif E resulted in changes in nucleotide binding indicating that a flexible network of hydrogen bonds between many distant regions of the protein, the RNA substrate, and the incoming nucleotide are responsible for specificity and catalysis (Cho *et al*., 2007). Moreover, further mutations in this region resulted in the transformation of a CCA-adding enzyme into a polynucleotide polymerase indicating a role for this region of the protein in the termination of nucleotide addition (Cho *et al*., 2007). Studies in our lab (Arthur, 2009) have shown the importance of motif E in the *Candida glabrata* class II tRNA nucleotidyltransferase as mutagenesis at position 244 results in cell death likely by altering the binding and orientation of the nucleotide triphosphate substrates.

1.3.3.6 Motif C

No specific roles have been assigned to motif C (Fig. 1-4) and its function in tRNA nucleotidyltransferase activity is not well understood. However, our group showed recently that a mutation in this region of the *Saccharomyces cerevisiae* enzyme resulted in decreased enzyme activity and a temperature-sensitive phenotype (Shan *et al*., 2008) suggesting that this domain may play a specific role in enzyme activity.

1.4 *Saccharomyces cerevisiae* tRNA nucleotidyltransferase

Characterization of various tRNA nucleotidyltransferases has been ongoing for almost 75 years (reviewed in Deutscher, 1973). Rether *et al*. (1974) provide one of the first detailed characterizations of this enzyme from baker's yeast. They showed K_M values of 450 μM and 260 μM for ATP and CTP, respectively. Later, Chen *et al*. (1990) reported similar K_M values of 560 μM and 180 μM for the two substrates. More recently, Aebi *et al*.(1990) have shown that yeast tRNA nucleotidyltransferase is essential by isolating a temperature-sensitive (ts) allele. *Saccharomyces cerevisiae* strain ts352 was unable to grow at 37°C, but exhibited normal growth at room temperature (22°C). Peltz *et al*. (1992) further showed that upon shift of this

temperature-sensitive strain to the restrictive temperature, protein synthesis stopped quickly as the pool of functional tRNAs (containing an intact 3'-CCA sequence) was rapidly reduced. It subsequently was shown that the ts phenotype resulted from a single G to A substitution in the *CCA1* gene resulting in a glutamate to lysine substitution at position 189 in the enzyme (Shan *et al.,* 2008).

Based on the available crystal structures of class II tRNA nucleotidyltransferases, E189 in the yeast enzyme is predicted to lie in motif C (Fig. 1-4) near the end of a β-strand where it supports a β-turn near the junction of the head and neck domains. The conversion of E189 to K resulted in reduced activity at both the permissive and restrictive temperatures *in vitro* and a 6°C lowering of melting temperature in the variant as compared to the native enzyme (Shan *et al.*, 2008). Replacing E189 with F, Q, or H showed a variety of structural and catalytic changes *in vitro* and differing growth phenotypes (Shan *et al*., 2008). The E189F variant showed reduced activity (approximately 25 fold less than native enzyme) and thermal stability, and like the E189K variant also exhibited the temperature-sensitive phenotype. The E189Q variant showed activity at about 40% of the native enzyme, no change in thermal stability *in vitro* and a 75% reduction in growth rate at 37°C. While the E189H variant showed no measurable change in thermal stability it showed a 13-fold reduction in activity and conferred a temperature-sensitive phenotype. Based on these results it was proposed (Shan *et al*., 2008) "that the E189F substitution altered the organization of the head and neck domains generally by disrupting (through lost hydrogen-bonding potential or through steric hindrance) a turn connecting a β-strand and an α-helix in the region of the yeast enzyme corresponding to Motif C". Given the important catalytic residues in the head and neck regions of the protein it would not be surprising if altering the local arrangement of this region could affect enzyme activity. Moreover, the wide range of effects conferred by the E189 substitutions did not distinguish between whether the temperature-sensitive phenotypes were caused by reduced thermal stability of the variant proteins or by partial defects in enzyme activity which only affected growth at higher temperatures.

To further explore the role of glutamate 189 in yeast tRNA nucleotidyltransferase structure and function and to investigate its role in the temperature-sensitive phenotype, UV mutagenesis was used to generate an intragenic suppressor (*cca1-E189F,R64W*) (Goring *et al*.,

2013). R64 of the yeast enzyme (Fig. 1-4) is found in a position corresponding to the end of a β-strand at the start of motif A (based on the available structure of the *B. stearothermophilus* enzyme). The R64W substitution restores the E189F protein to an active conformation without restoring thermal stability, suggesting an important structural association between residue 64 in motif A and residue 189 in motif C. The protein encoded by the *cca1-E189F,R64W* allele shows increased activity at the restrictive temperature suggesting that it is the reduced activity of the *cca1-E189F* variant and not its altered stability that confers temperature-sensitivity (Goring *et al*., 2013).

1.5 This study

Although reduced activity has been shown in the E189F variant with a restoration of this activity in the R64WE189F variant, it is unknown why the levels of activity change. Substrate binding or catalysis could be effected in either case. Here, a detailed enzymatic characterization is performed to determine what parameters of enzyme activity (k_{cat} or K_M for tRNA) are altered. A better understanding of the roles of these amino acids in enzyme structure and function may allow us to define more precisely the roles of R64 and E189 and by extension of motifs C and E, respectively.

2.0 MATERIALS AND METHODS

2.1 Strains and Plasmids

Escherichia coli strains BL21 (DE3) and XL2-Blue were purchased from Stratagene for protein expression and DNA manipulations, respectively. Protein expression was carried out using the inserts of interest in a modified pGEX-2T (GE Healthcare) vector (Shan *et al*., 2008) containing an added *Sal*I site downstream of the existing *Bam*HI restriction site. Plasmid pmBsDCCA (Oh and Pace, 1994), kindly provided by Dr Alan Weiner, was used for the production of a tRNA substrate lacking its terminal adenine residue.

2.2 Buffers, solutions and media

PBS (Phosphate Buffered Saline) (Sambrook *et al*., 1989)	8 g/L NaCl, 0.2 g/L KCl, 1.44 g/L Na_2HPO_4, 0.24 g/L KH_2PO_4
Thrombin Digestion Buffer (Modified from Arthur, 2009)	500 mM Tris pH 7.7, 1.5 M NaCl, 25 mM $CaCl_2$
TBE (Tris-Borate-EDTA) (4L) (Sambrook *et al*., 1989)	120 g Tris, 62 g Boric acid, 40 mL 0.5 M EDTA (pH 8)
YT (Sambrook *et al*.,1989)	0.8% Tryptone, 0.5% Yeast extract, 0.5% NaCl
Protein Running Buffer (Modifed from Sambrook *et al*., 1989)	72 g/L glycine, 15 g/L Tris, 5 g/L SDS
Solution A (Wong *et al.*, 2000)	0.05% Coomassie blue, 25% isopropanol, 10% acetic acid
Solution B (Wong *et al.*, 2000)	0.005% Coomassie blue, 10% isopropanol, 10% acetic acid
Solution D (Wong *et al.*, 2000)	10% acetic acid, 10% isopropanol

2.3 Protein Purification

2.3.1 Protein Expression

An overnight culture (10 mL) of BL21 (DE3) cells expressing native or variant tRNA nucleotidyltransferase was inoculated into a Fernbach flask containing 1.3 L of YT medium containing 100 mg/mL ampicillin (Goldbio). The culture was incubated with shaking at 37°C until the optical density (OD_{600}) reached 0.4-0.7 absorbance units. Once ready, 650 µL of 1M IPTG (Goldbio) and 25 mL of 10.4% lactose (Bioshop) were added to each Fernbach flask to induce protein expression (16 hours at 18ºC for the plasmids used for expressing native, R64W, or R64WE189F protein or three days at 4ºC for the plasmid expressing E189F protein). Then, the cells were harvested by centrifugation at 6 000 rpm (JA-10 rotor) for 20 minutes. Cell pellets were stored at -80°C until needed. All subsequent steps were carried out on ice or at 4ºC.

2.3.2 Protein Extraction

Cell pellets were thawed on ice and resuspended by vortexing in lysis buffer (1XPBS + 1mM EDTA, modified from Shan *et al*, 2008) using 2 mL lysis buffer/g of cell pellet. Cells were lysed by passage three times through a French Pressure Cell (FA-078) at 16 000 PSI. The lysate was cleared by centrifugation at 18 000 rpm (JA-20 rotor) for 1 h.

2.3.3 GST-protein purification

A column was packed with 1 mL of Glutathione Sepharose 4B (Goldbio) resin and washed with 100 mL of PBS at a flow rate of 1 mL/min. The column was equilibrated with running buffer (see below) and the cleared lysate (20-25 mL) was cycled through the column for 16 h at 4°C at a flow rate of 4.6 mL/min. The column was washed with 1 L of PBS at a flow rate of 12 mL/min and the eluant discarded. Subsequently, 100 mL of PBS containing 15 mM glutathione were added and 1 mL fractions were collected at a flow rate of 1 mL/min at room

temperature. The amount of protein contained in each fraction was compared by carrying out SDS-polyacrylamide gel electrophoresis (see section 2.4.1) on 16 µL aliquots of each fraction. The fractions showing the greatest amount of the GST fusion protein (typically 10) were pooled and dialyzed overnight in 50 kDa molecular weight cut off dialysis tubing (SpectrumLabs) against 5 L of 10 mM Tris buffer (pH 8) containing 0.0002 mg/mL thrombin (GE Healthcare, 500 units/mg) to remove the GST tag. The next day, the contents of the dialysis bag were passed through the GST affinity column three times at a flow rate of 4.6 mL/min to remove the released GST-tag and any undigested protein. The flow through from the final GST affinity column was pooled and an aliquot analyzed by SDS-PAGE to determine its purity. The pure protein was stored as 200 µL aliquots at -80°C. Protein concentrations were determined by Bradford assay (section 2.4.4).

2.3.4 GST Column Equilibration

The Glutathione 4B Sepharose resin was first incubated with one half-volume of 25 mM glutathione for five minutes. Then, after removing the glutathione, the resin was washed with an equal volume of PBS. Subsequently, the resin was mixed with one half volume of 6M Guanidinium-HCl (Gd-HCl), stirred with a glass-rod and incubated for two minutes. After removal of the 6M Gd-HCl, the resin was washed again with one volume of PBS. Then, following another five minute incubation in one half volume of 25 mM glutathione, an equal volume of 20% ethanol was added for storage of the resin at 4°C. Finally, before use the resin was prewashed with 10 volumes of PBS.

2.4 Protein Concentration Characterization

2.4.1 SDS-PAGE

A 13.5% (v/v) polyacrylamide (29:1 acrylamide to *bis*-acrylamide ratio) resolving gel in 0.5 mM Tris buffer (pH 8.8) with 10% (v/v) SDS was prepared and a 4.5% (v/v) polyacrylamide (29:1 acrylamide to *bis*-acrylamide ratio) focusing gel in 1.5 M Tris buffer (pH 6.8) with 10% SDS was layered on top. TEMED (10 µL/mL) and 10% (v/v) ammonium persulfate (100 µL/mL) were used as reaction catalysts for polymerization in both cases. Electrophoresis typically was carried out using a 50 mM glycine-50 mM Tris buffer (pH 8.8) containing 10% SDS for 45 minutes at 200 mV. Every 16 µL sample had 4 µL of loading dye containing 10% SDS (w/w), 50% glycerol (v/v), 25% β-mercaptoethanol (v/v) and 0.25% bromophenol blue (w/w) in 300 mM Tris-HCl (pH 6.8) added before the samples were placed in a boiling water bath for two minutes. An unstained mass ladder (Thermo-Scientific) was used in each experiment.

2.4.2 SDS-gel Staining and Destaining (Wong *et al*., 2000)

Staining and destaining were done with solutions A, B and D (see above in section 2.2). The SDS-gel was heated in a micro-wave oven for 1 minute with solution A and incubated on a shaker for 10 minutes. Then, the gel was washed with distilled water and the procedure was repeated for solutions B and D.

2.4.3 Bradford Assay

A 2 mg/mL bovine serum albumin (BSA) (ICN Biochemicals) standard solution was prepared by dissolving 20 mg of BSA in 10 mL of distilled water (dH_2O). By measuring the absorbance of the BSA solution at 280 nm, the concentration was verified by applying the Beer-Lambert law with a molecular weight of 66 580 g/mol using a molar extinction coefficient of 43 824 M^{-1} cm^{-1} with a cuvette of 1 cm path length. BSA standards of 1 µg/mL, 2 µg/mL, 4 µg/mL,

6 µg/mL, 8 µg/mL, 9 µg/mL and 10 µg/mL were prepared in dH_2O from the standard BSA solution. A volume of 800 µL was transferred from each standard into 200 µL of Bradford dye in a microfuge tube. The dilutions were incubated at room temperature for 10 minutes before taking their absorbance at 595 nm. The blank used was a volume of 800 µL of dH_2O in 200 µL of Bradford dye.

2.4.4 Ultraviolet-Visible (UV-Vis) Spectrophotometry

The UV-Vis spectra were obtained using a Varian Cary 100 Bio UV-Vis spectrophotometer. Several dilutions of each sample were prepared. Frozen samples were thawed on ice and centrifuged briefly. The UV-Vis spectral range scanned was from 300 nm to 200 nm at a scan rate of 60 nm/min. The average time was one second with a data interval of 0.1 nm. A spectrum of the PBS buffer was taken and used for baseline correction.

2.5 Enzyme Assays

2.5.1 Run-off Transcription of tRNA-NCC

An amount (~5-10 µg) of plasmid pmBsDCCA was digested with *Bbs*I at 37°C for two hours. An equal volume of phenol was added with vortexing to stop the reaction. A phenol extraction (see section 2.5.3) was performed followed by an ethanol precipitation (see section 2.5.4) with resuspension in RNAse-free distilled water. The run-off assay contained 20 µL 5X Transcription buffer (Thermo Scientific), 5 µL 10 mM CTP (Thermo Scientific), 5 µL 10 mM UTP, 5 µL 10 mM ATP, 5 µL 1 mM GTP, 4 µL of RNase Secure (Ambion) and the linearized plasmid in a final volume of 92 µL. This mixture was heated at 70°C for 10 min. To start transcription, 5 µL of α^{32}P-GTP (3000 Ci, 10 mCi/mL) and 3 µL of T7 RNA polymerase (20 units/µL, Thermo Scientific) were added. The mixture was incubated for 2-3 hours at 37°C. The reaction was stopped by adding 200 µL of phenol and vortexing. Phenol extraction and ethanol precipitation were performed (see sections 2.5.3-2.5.4). Electrophoresis was carried out in a 7 M

urea 20% acrylamide (29:1 acrylamide:Bis acrylamide) 1X TBE gel to ascertain the purity of the preparation.

2.5.2 Preparation of yeast tRNA

A total of 10 mg of baker's yeast tRNA (Roche, 10 109 495 001) was resuspended in 360 µL of nuclease-free dH_2O and 40 µL of 1 M NaOH by vortexing. An equal volume of phenol was added and phenol extraction was performed (see section 2.5.3) followed by ethanol precipitation (see section 2.5.4). The sample was resuspended in 200 µL of 4 M Tris-HCl (pH 8.0) by vortexing and the solution was incubated at 37°C for 1.5 hours to remove any amino acids that may have remained attached to the 3' ends of the tRNAs (Sarin and Zamenick, 1964). Then, 55 µL of 3M NaCl was added and the ethanol precipitation repeated. The plasmid DNA was resuspended in 300 µL of 200 mM Tris-HCl (pH 9.0) and 0.5 mg of snake venom phophodiesterase (Sigma-Aldrich, P3243) was added to trim the CCA sequence from the 3' end of the tRNA at room temperature for 1 hour (Chiemprasert and Philipps, 1976). Subsequently, four phenol extractions, two ether extractions and an ethanol precipitation were performed. The tRNA was resuspended in 21 µL of RNase-free dH_2O and stored at -80°C until used.

2.5.3 Phenol Extraction

Phenol extractions were routinely used to remove protein from the nucleic acid samples. If no salt was present in the sample, sodium acetate was added to a concentration of 300 mM and a volume of phenol equal to the aqueous phase was added. The tube was vortexed and then centrifuged for five minutes in an Eppendorf centrifuge at 4°C. The aqueous layer was collected avoiding any material at the interface between the aqueous and phenol layers and another equal volume of phenol was added. The cycle was repeated as necessary until no material was apparent at the interface between the phenol and aqueous layers.

2.5.4 Ethanol Precipitation

Nucleic acid samples were typically concentrated by ethanol precipitation. If no salt was present in the sample, sodium acetate was added to a concentration of 300 mM and two volumes of 99% ethanol were added with vortexing. Then, the tube was incubated at -20ºC for a day or at -70ºC for a minimum of 30 minutes. The tubes were centrifuged for 30 minutes in an Eppendorf centrifuge at 4°C. The supernatant was removed and the DNA pellet was washed with 80% ethanol and the DNA pellet was desiccated for 30 minutes before resuspension in the appropriate amount of liquid.

2.5.5 Activity Assays

The procedure of Leibovitch *et al* (2013) was used to measure enzyme activity. In brief, each 10 µL reaction contained 100 mM glycine buffer (pH 9), 10 mM $MgCl_2$, 1 mM ATP, 0.4 mM CTP, 1 µL radiolabelled transcript (typically 0.1 to 0.3 pmoles), and 50 ng of protein. (Given the low level of activity in the E189F variant, 200 ng of this protein was required). To limit the amount of radiolabelled tRNA used in each assay the tRNA substrate concentration was varied by adding increasing amounts of unlabelled yeast tRNA for final concentrations ranging from 12 – 1000 µM. Multiple reactions could be combined in a single Eppendorf tube if many time points were to be sampled. The samples were heated at 60°C for 10 minutes and cooled to room temperature before the protein was added and mixed with a pipette tip. Ten µL aliquots were removed at the appropriate time points and added to 10 µL Peattie's loading dye (Peattie, 1979) at 70°C for 10 minutes to stop the reaction with subsequent storage on ice. Reaction progress was measured by phosphorimaging of the samples after electrophoresis for 18 h at 2000 V on a 50 cm 7 M urea/20% polyacrylamide/1X TBE gel in 1X TBE buffer. The gel was pre-run at 1500 V for 30 minutes in 1X TBE before the samples were loaded.

2.5.6 Phosphorimaging

After electrophoresis, a Geiger-Muller detector was utilized to locate the location of the radiolabeled tRNA in the gel such that this region of the gel could be excised, wrapped in plastic wrap (Roll-O-Sheets) and placed under a phosphorimaging screen in a cassette. The cassette was closed and left for a day. Then, the phosphorimaging screen was removed from the cassette and brought to a Typhoon TRIO Variable Mode Imager (GE Healthcare) to develop an image. With the densitometer of the ImageQuantTL 1D, the band intensities of product and reactant were measured.

2.5.7 Grafit

GRAFIT Version 7 (http://www.erithacus.com/grafit/) a curve fitting software program for Windows, was used to build Michaelis-Menten graphs of the initial velocity data collected from the enzyme activity assays. The program gave the apparent K_M and V_{max} values.

2.6 Molecular Modelling

SWISS-MODEL (Biasini *et al*., 2014), a protein homology server, was used to build models of the enzyme variants from their amino acid sequence. The *Thermotoga maritima* tRNA nucleotidyltransferase was selected as the best template for modelling after comparison of the GMQE and QMEAN4 scores of the four elucidated tRNA nucleotidyltransferase crystal structures. Pymol (http://www.pymol.org/) was used to visualize the enzymes.

3.0 RESULTS

The native, E189F, R64W and R64WE189F variants were expressed and purified by PKS. PKS carried out the subsequent characterization of the native, E189F and R64WE189F variants. Matthew Leibovitch characterized the R64W variant and repeated the enzymatic characterization of the native, E189F and R64WE189F variants. Matthew's data are included in the results and discussion to show the highest level of statistical significance. PKS performed all of the molecular modelling.

3.1 Protein Purity and Structure

Multiple modifications were required to develop a protocol which resulted in good yields of the E189F variant. However, incorporating these modifications resulted in the development of a protein purification scheme that generated protein of sufficient yield (Table 3-1) and purity (Figures 3-1 and 3-2) for enzymatic and biophysical characterization.

Table 1: Amounts of purified tRNA Nucleotidyltransferases

tRNA-NT	Concentration (µg/mL)	S_E (µg/mL)	Total Protein (mg)
Native	252	53	2.5
E189F	282	75	2.8
R64W	1544	686	15
RWEF	341	34	3.4

Cycling the cleaved protein through the glutathionine affinity column multiple times resulted in elimination of the GST-tag from the protein (Fig. 3-1). Each cycle through the glutathione affinity resin resulted in an enrichment of the tRNA nucleotidyltransferase and a loss of GST (compare lanes 3, 4 and 5). The final lane (lane 5) shows a sufficient yield of pure protein of the expected molecular weight with little contaminating protein.

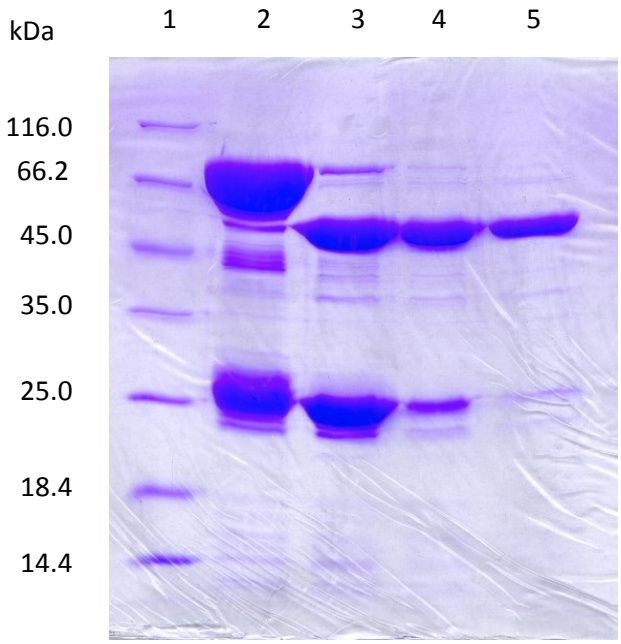

Figure 3-1. SDS-PAGE of native tRNA nucleotidyltransferase before and after thrombin cleavage and purification on the glutathione affinity column. Lane 1, Molecular weight standards (Thermo-Scientific); Lane 2, soluble protein from heterologous expression after affinity purification; Lane 3, protein collected from first passage through glutathione affinity column; Lane 4, protein collected from second passage through glutathione affinity column; Lane 5, protein collected from third passage through glutathione affinity column.

The high level of purity (approximately 80%) seen for the native tRNA nucleotidyltransferase also was seen with the variant proteins with only minor bands reflecting contaminating GST-tag and uncut protein present at approximately 25 kDa and 80 kDa, respectively (Fig. 3-2). The modifications introduced to the purification scheme for the E189F variant (longer expression times at a lower temperature) resulted in increased yields of the E189F variant as compared to the yields generated using the original expression conditions (data not shown).

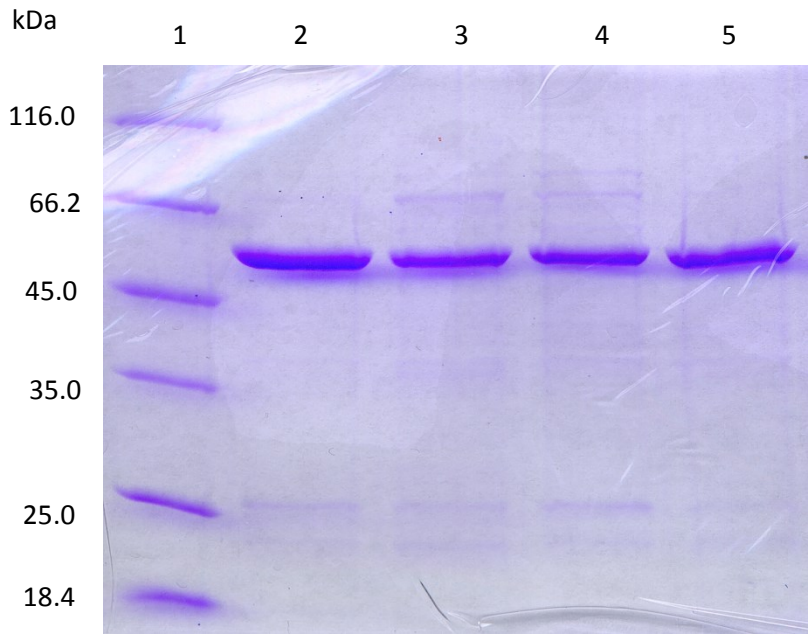

Figure 3-2. SDS-PAGE gel of the purified tRNA nucleotidyltransferases. Lane 1 shows the molecular weight ladder while lanes 2-5 show the native, E189F, R64WE189Fand R64W tRNA nucleotidyltransferases, respectively. The faint bands at 25 kDa and 85 kDa represent the cleaved GST tag and residual uncut fusion protein, respectively.

We previously have shown that tRNA nucleotidyltransferase can be purified with tRNA associated with it (Leibovitch *et al*., 2013), so all samples were exposed to UV-Visible spectroscopy to see if a signal suggestive of tRNA (absorbance ~260 nm) could be observed. Both the R64W and R64WE189F variants showed peaks suggestive of tRNA copurifying with the enzyme (Figure 3-3).

Figure 3-3: UV-Visible spectra of tRNA nucleotidyltransferase variants

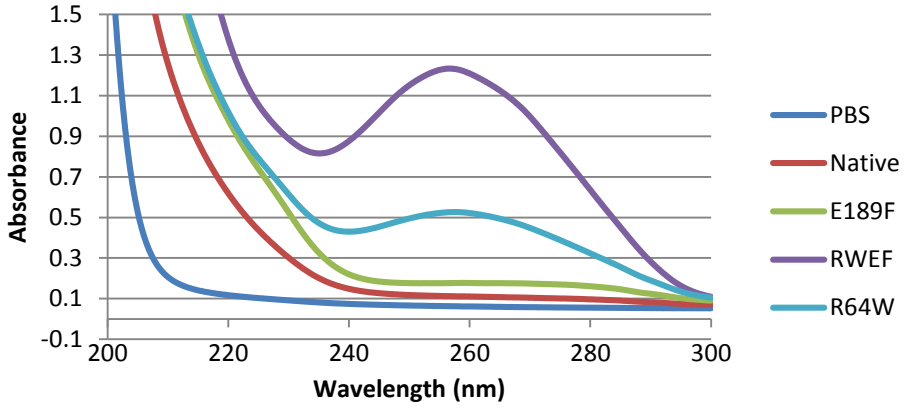

Proteins were diluted to 100 µg/mL according to their concentrations calculated by the Bradford assay. The spectrum of the buffer, PBS, is also shown.

3.2 Enzyme Assays

A kinetics assay was developed to characterize the effects of the amino acid changes on enzyme activity: specifically the addition of the adenosine to a tRNA-NCC transcript. Based on previous studies on the yeast tRNA nucleotidyltransferase (Chen *et al*, 1990), the concentrations of CTP (0.4 mM) and ATP (1mM) were set in the range of twice their previously determined K_M values, 0.26 mM and 0.45 mM, respectively (Rether *et al*., 1974). Every series of reactions contained a positive control of undiluted native enzyme and a negative control of boiled native enzyme. A series of reactions was carried out to determine the best time points to use to calculate the initial velocity (Fig. 3-4). A total reaction time of five minutes was chosen with time points taken at 20 seconds, , 1 minute and 5 minutes. An observable linearly proportional relationship between product formation and duration of reaction was established between 10% and 30% product formed (data not shown). Taking the 14 day half-life of the 32-phosphorus radioactive signal into account, all lanes of product and reactant were baseline corrected.

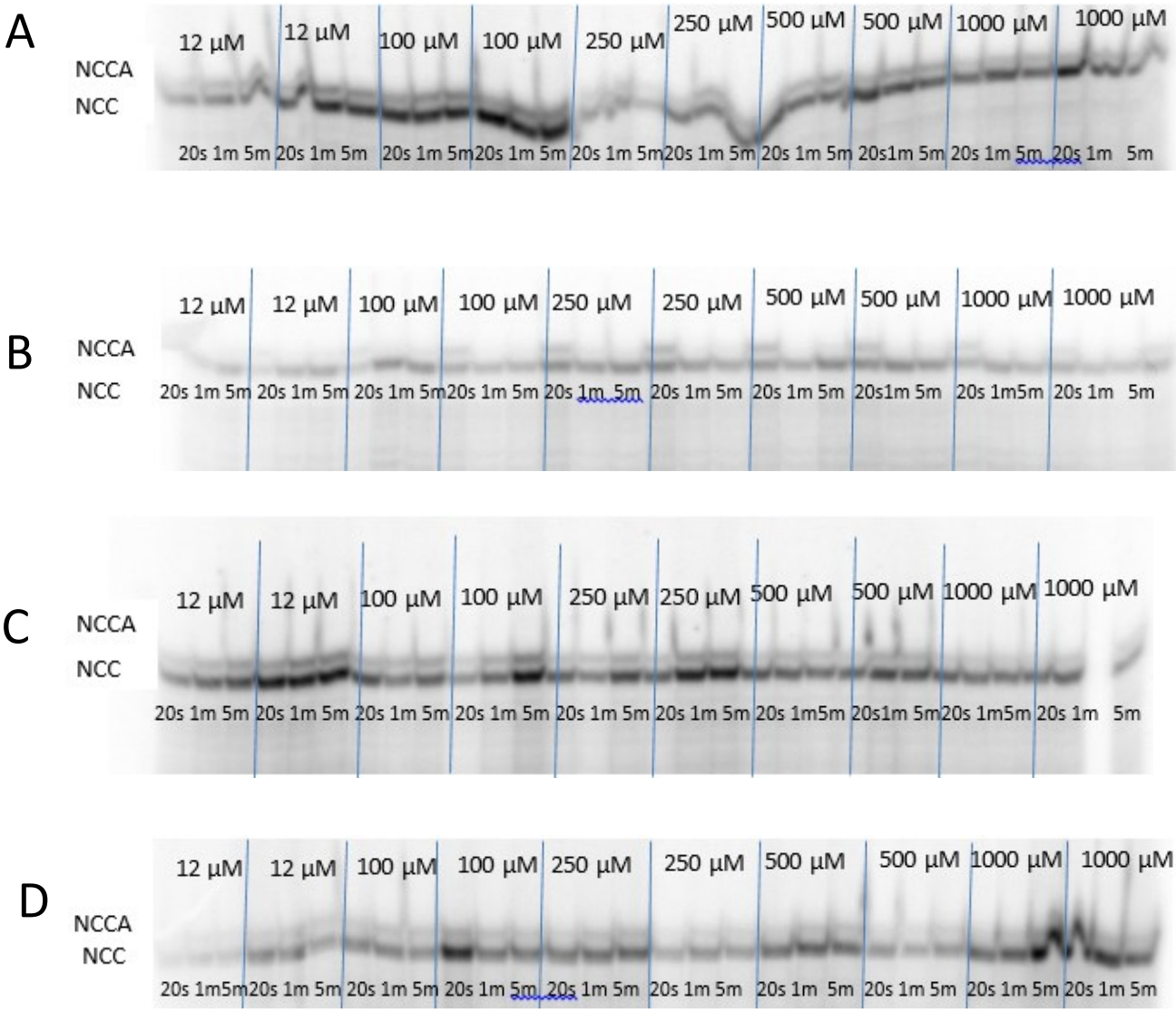

Figure 3-4. Time courses for conversion of tRNA-NCC to tRNA-NCCA. The values above the data indicate the amount of unlabelled yeast tRNA added to each sample and the reaction times are indicated below each lane. A) native enzyme, B) E189F, C) R64WE189F, D) R64W.Grafit software was used to plot the initial rates of adenosine addition to the tRNA-NCC substrate. Figure 3-5 shows the GraFit Michaelis-Menten kinetics derivation for all tRNA nucleotidyltransferase enzymes.

Analysis of these results shows a standard error of at most 30% for K_M while k_{cat} has an even lower standard error of at most 13%. The Michaelis constant (K_M) for tRNA binding was

about 2 µM for all variants of tRNA nucleotidyltransferase (see Table 3-2). However, the k_{cat} did vary among the enzymes. The k_{cat} was highest for the native (1.2 s^{-1}) and R64W (0.93 s^{-1}) proteins and weakest for E189F ($6.8x10^{-2}$ s^{-1}). The R64WE189F enzyme had an intermediate k_{cat} (0.10 s^{-1}) that approached that of the native and R64W proteins (within the same order of magnitude).

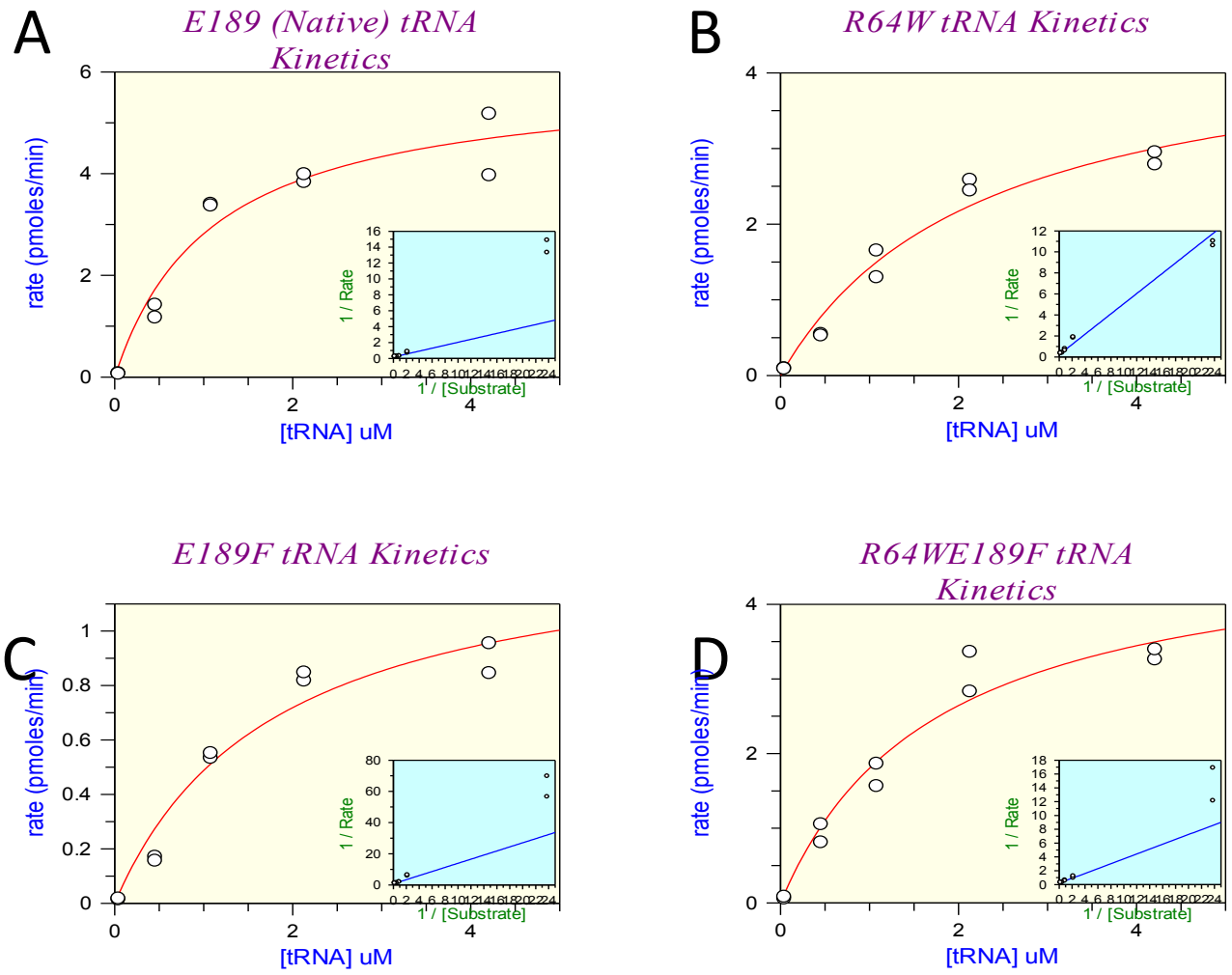

Figure 3-5. Effect of increasing tRNA concentration on tRNA nucleotidyltransferase activity. Duplicate activity assays done for five concentrations of tRNA (0.005 µM, 0.42 µM, 1.05 µM, 2.1 µM, 4.2 µM) at three reaction times (20s, 1 min, 5 min). A) Native, B) E189F, C) R64W, D) R64WE189F.

Although the changes in K_M are small, when they are factored into the calculation of catalytic efficiency they highlight more clearly the differences between the native and variant enzymes and correlate well with the observed phenotypes. For example, with respect to the native enzyme (1.1 s^{-1} μM^{-1}), the catalytic efficiency of the E189F variant is reduced more than 100-fold to $9.4x10^{-3}$ s^{-1} μM^{-1} and cells bearing this mutation are temperature-sensitive. In contrast, the R64W variant has a catalytic efficiency (0.42 s^{-1} μM^{-1}) that is approximately 40% that of the native enzyme and cells bearing this mutation are viable at the restrictive temperature. Most interesting is the R64WE189F variant which shows catalytic efficiency ($5.9x10^{-2}$ s^{-1} μM^{-1}) which is 6-fold higher than that of the E189F variant such that the cells are viable at the restrictive temperature. However, in all of these cases it is apparent that the changes in k_{cat} contribute most to the changes in catalytic efficiency.

Table 3-2: Apparent Kinetic Constants of tRNA Nucleotidyltransferases

tRNA-NT	K_M (μM)	S_E	k_{cat} (s^{-1})	S_E	k_{cat} / K_M (s^{-1} μM^{-1})	S_E
E189	1.1	0.35	1.2	0.14	1.1	0.36
E189F	1.8	0.56	$1.7x10^{-2}$	$9.3x10^{-3}$	$9.4x10^{-3}$	$3.8x10^{-3}$
R64WE189F	1.7	0.50	0.10	$1.2x10^{-2}$	$5.9x10^{-2}$	$1.8x10^{-2}$
R64W	2.2	0.62	0.93	0.12	0.42	0.13

3.3 *Thermotoga maritima* homology model

Images of the tRNA nucleotidyltransferase variants (Fig. 3-6) were taken with Pymol from a homology model generated by using the SWISS model server as described in Materials and Methods. Only the amino terminal portion of the protein containing motifs A to E is shown.

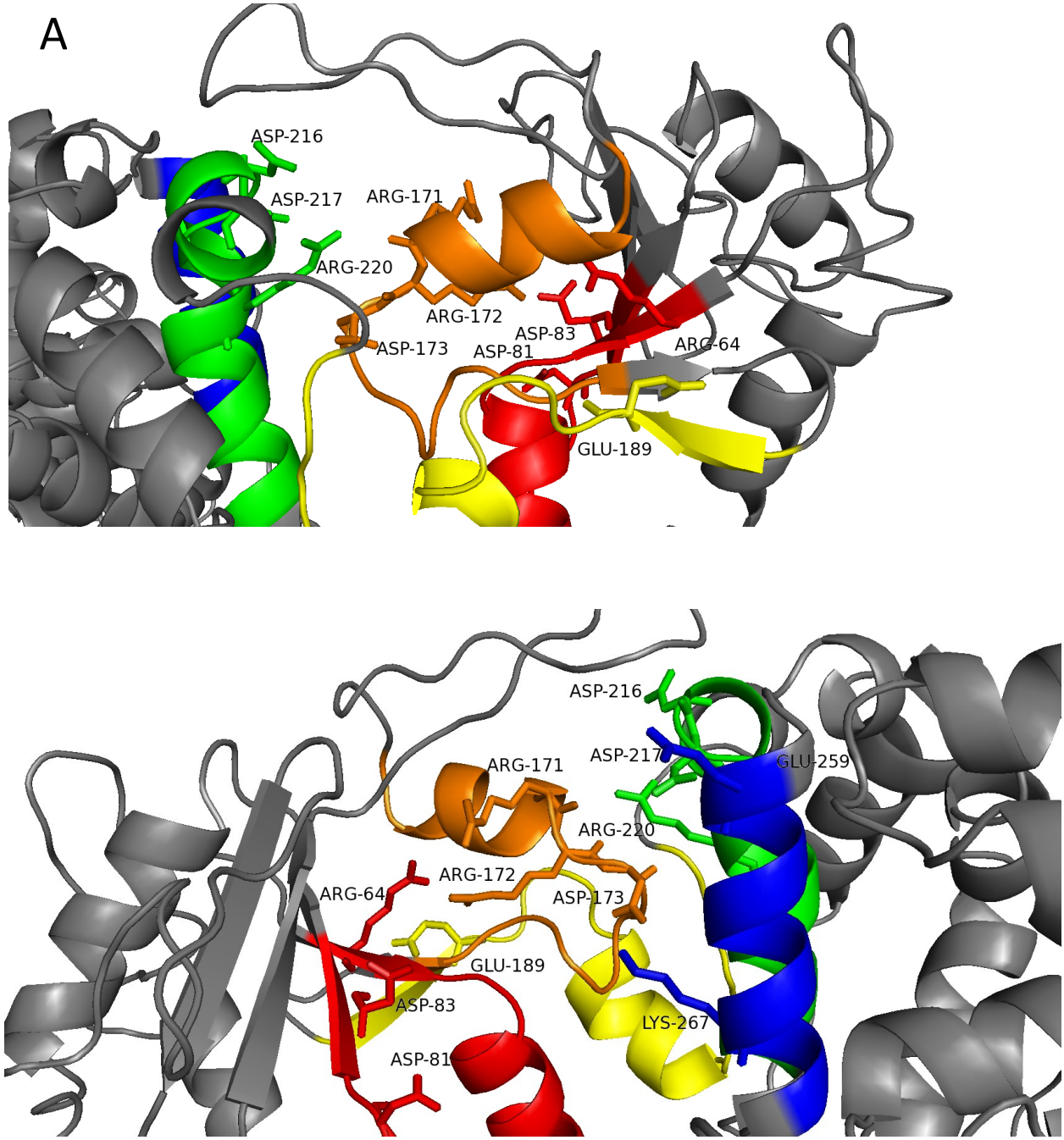
A
ASP-216
ASP-217
ARG-171
ARG-220
ARG-172
ASP-83
ASP-173
ASP-81
ARG-64
GLU-189
ASP-216
ASP-217
GLU-259
ARG-171
ARG-220
ARG-172
ARG-64
ASP-173
GLU-189
ASP-83
LYS-267
ASP-81

B

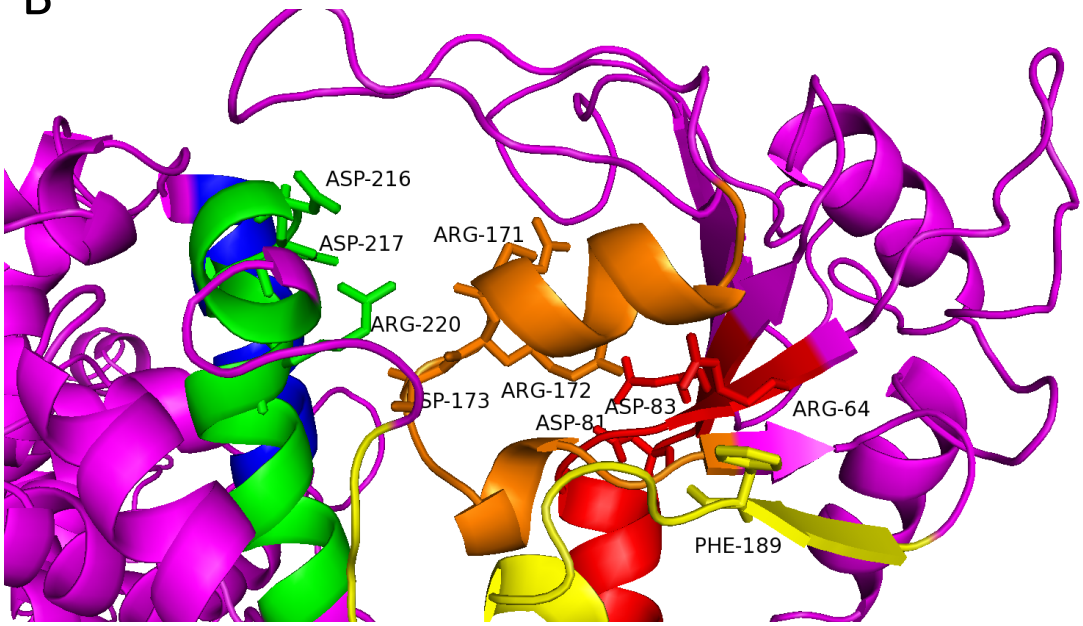
ASP-216
ASP-217
ARG-171
ARG-220
SP-173
ARG-172
ASP-83
ASP-81
ARG-64
PHE-189

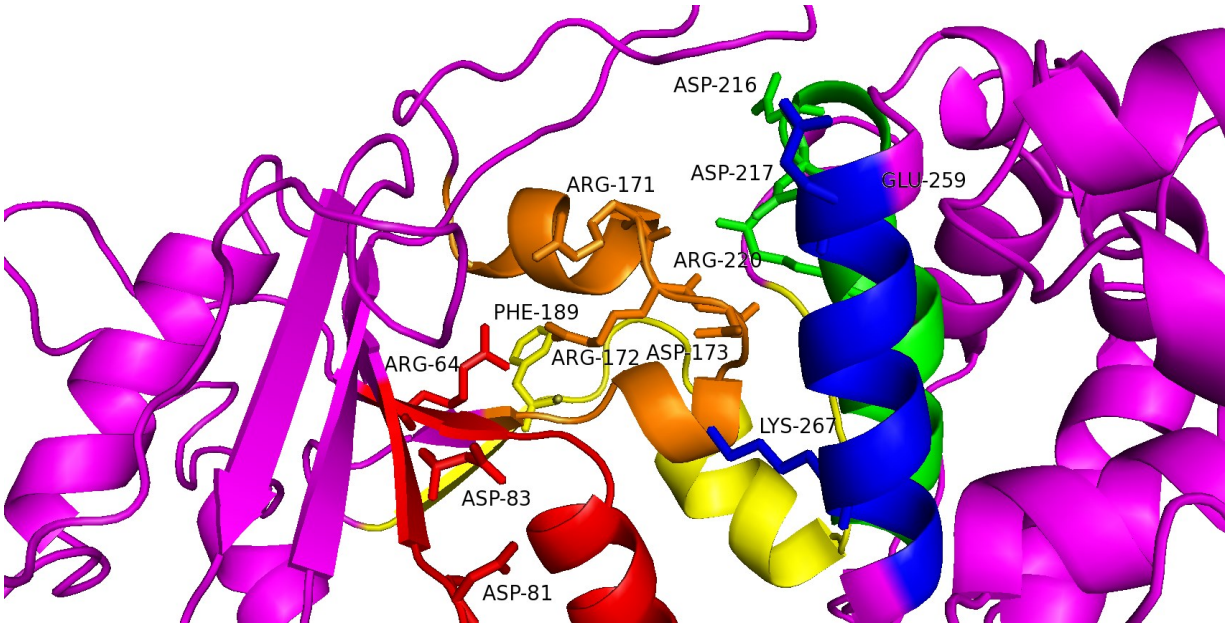
ASP-216
ASP-217
GLU-259
ARG-171
ARG-220
PHE-189
ARG-64
ARG-172
ASP-173
LYS-267
ASP-83
ASP-81

C

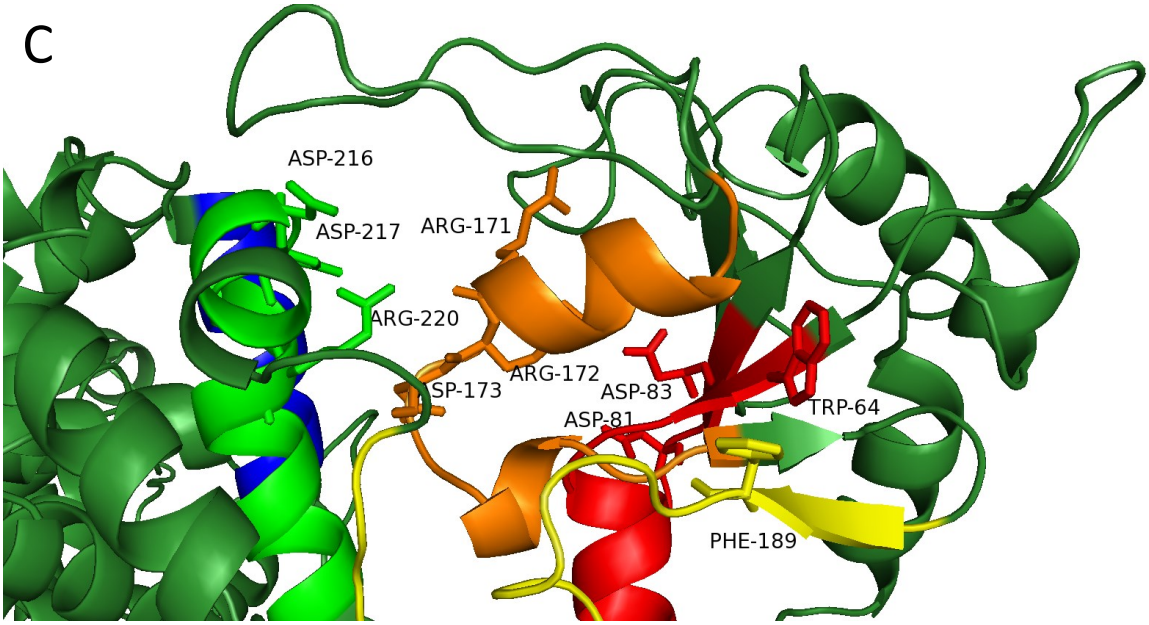
ASP-216
ASP-217
ARG-171
ARG-220
ARG-172
SP-173
ASP-83
ASP-81
TRP-64
PHE-189

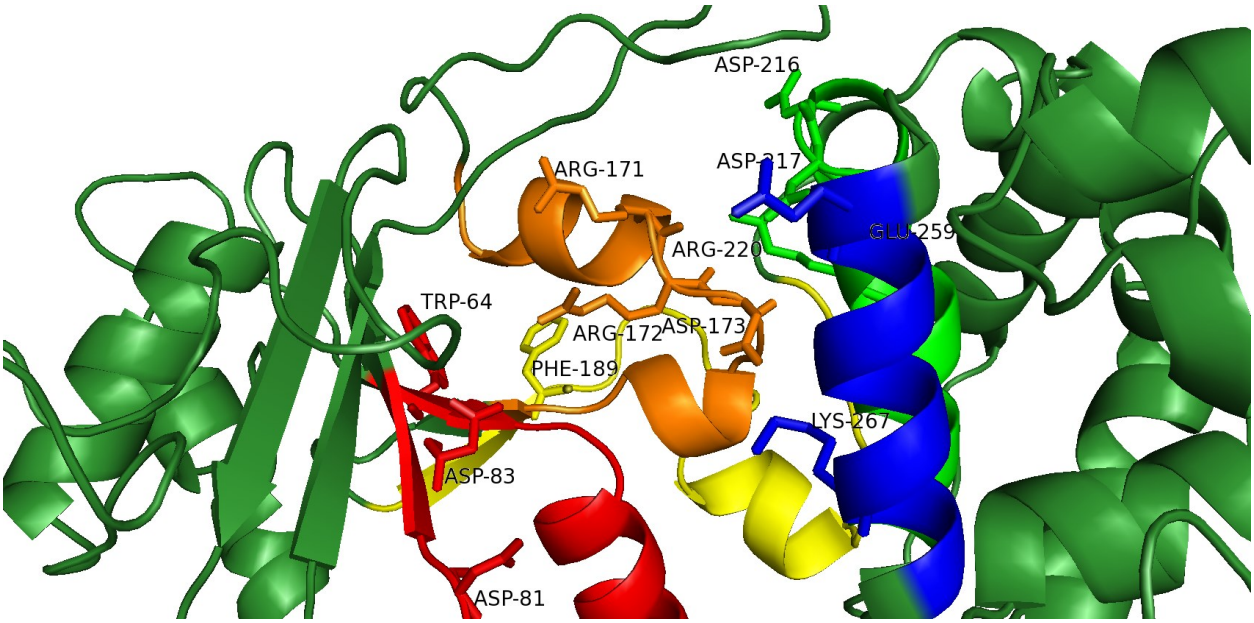
ASP-216
ARG-171
ASP-217
GLU-259
ARG-220
TRP-64
ARG-172
ASP-173
PHE-189
LYS-267
ASP-83
ASP-81

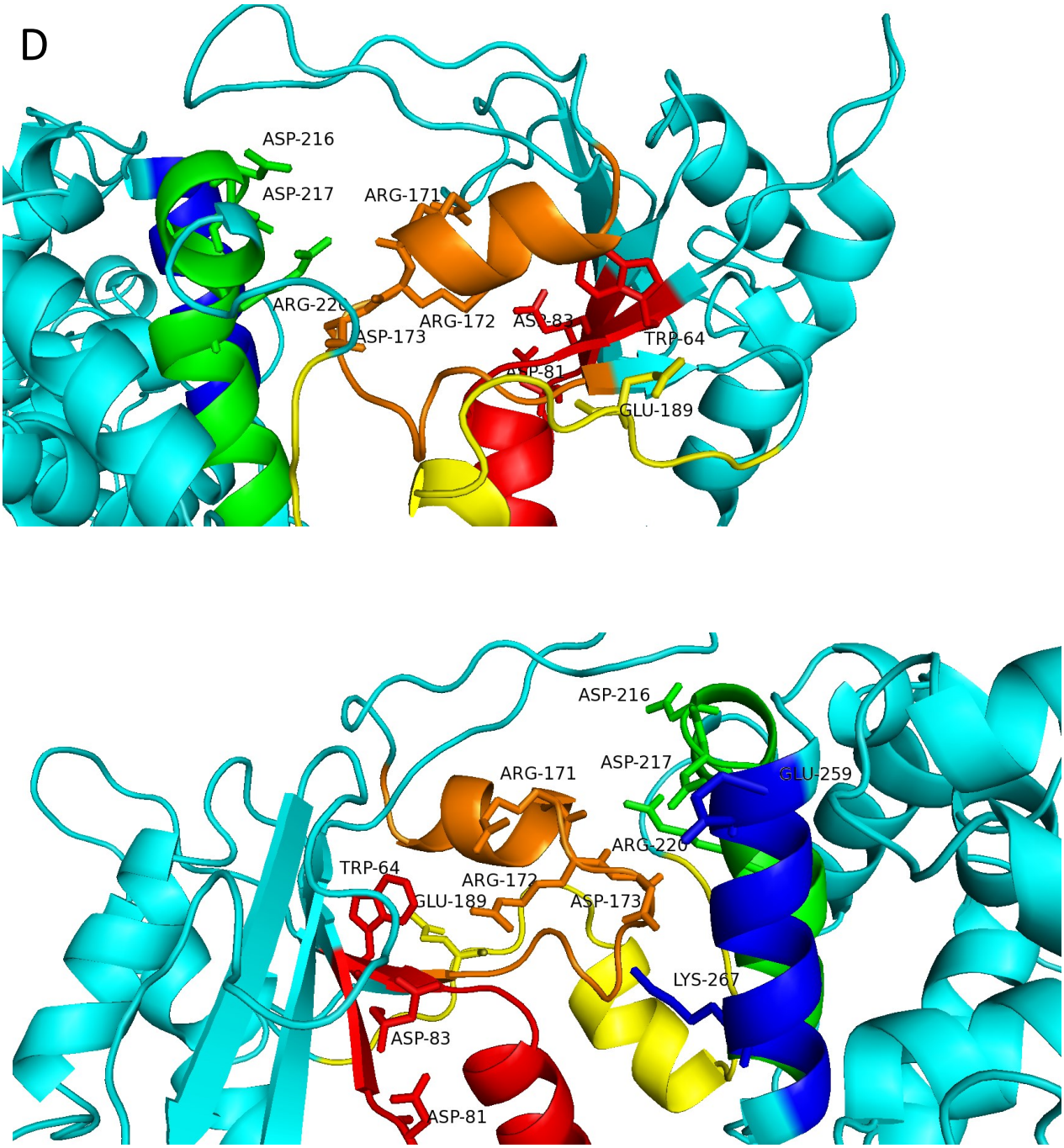

Figure 3-6. Models of native and variant yeast tRNA nucleotidyltransferases. SWISS-MODEL software (Biasini *et al.*, 2014) was used to model the native and variant yeast tRNA nucleotidyltransferases based on the existing *Thermotoga maritima* protein (3H38, Toh *et al.*, 2009). Images were manipulated in PyMol (http://www.pymol.org/). Positions 64 and 189 along with the known catalytic residues of motif A (E81 and E83), motif B (R171, R172 and

D173) and motif D (D216, D217 and R220) are shown as sticks. Regions corresponding to motifs A to E are shown in red, orange, yellow, green and blue, respectively. Panel A, native enzyme; Panel E189F variant; Panel C, R64WE189F; Panel D, R64W.

4.0 DISCUSSION

Motif C is the least well characterized of all of the conserved domains in class II tRNA nucleotidyltransferases. The identification of a temperature-sensitive mutation mapping to this region of the *Saccharomyces cerevisiae* enzyme (Aebi *et al*., 1990) affords an excellent opportunity to explore the role of this domain in enzyme structure and function. Moreover, the identification of a suppressor mutation in motif A that eliminates the temperature-sensitive phenotype (Goring *et al*., 2013) provides the chance to explore the organization and interaction of these two domains.

4.1 Purification of *Saccharomyces cerevisiae* tRNA nucleotidyltransferase

The purification scheme developed by Goring *et al*. (2013) proved effective in generating heterologously expressed tRNA nucleotidyltransferase of sufficient purity and quantity for further characterization (Table 3-1, Fig. 3-1, Fig. 3-2). Specifically, using multiple cycles on the glutathione column resulted in removal of almost all of the GST tag from the thrombin-digested protein (Fig. 3-1). Intriguingly, the R64W variant gave a much greater yield of protein (Table 3-1), possibly due to a conformational change that favors increased solubility or better binding to the GST column. The previous study (Goring *et al*., 2013) showed that E189F gave a much lower yield of protein than the native enzyme. We found this to be the case under standard expression and purification conditions (data not shown) and so adapted the expression and purification conditions such that the protein was expressed at a lower temperature (4^{o}C vs 15^{o}C) and for a longer time (16 hours vs 72 hours). By incorporating these changes, the low thermal stability of the protein (Goring *et al.*, 2013) was counteracted to allow better expression comparable to that of the native (Table 3-1).

4.2 Structural characterization

Both the R64W and R64WE189F variants showed an increase in absorbance at 260 nm as compared to the native and E189F variants. It previously has been shown (Leibovitch *et al*., 2013) that an increase in A_{260} can result from tRNA that remains associated with the tRNA

nucleotidyltransferase during protein purification. Even assuming that all of the A_{260} absorbance was due only to the tRNA associated with the protein, the largest amount of tRNA associated would be in the range of 1.92 to 20.8 pmoles given that 1 mg/ml tRNA has an A_{260} of 24 (Yue et al., 1998). This represents a 1/10 to 1/2 ratio of tRNA to protein in the protein fractions. Given that only 4.12 pmoles of protein were added to each assay this means that a negligible amount of tRNA was added even in the R64W and R64WE189F assays. This likely had little effect on the overall reaction given that even for the reaction with the lowest added substrate concentration 12 pmoles of yeast tRNA were added. Therefore, no efforts were made to separate any residual tRNA from any of the protein preparations.

As the increase in absorbance was seen with the two variants that contained the additional tryptophan residue which absorbs at 260 nm it cannot be formally excluded that this amino acid alone is directly responsible for the change in absorbance. Given that the protein has only five tryptophan residues at positions 69, 293, 443, 511 and 522 (Fig. 1-4) it is interesting that adding an additional tryptophan (W64) close to W69 resulted in this dramatic increase. However, comparing the models of the native enzyme and that of the R64W variant (Fig. 3-6) suggests that location of the additional tryptophan at a more solvent exposed site near the active site plays a role in the higher absorbance. Moreover, the relative 260/280 ratios for the R64W and R64WE189F variants are 1.62 and 1.90, respectively suggesting that it is not simply this new tryptophan residue that results in the increase in absorbance but that there also is a change in some aspect of the overall conformation of the protein or in how the protein interacts with the tRNA substrate. Leibovitch *et al*. (2013) argued that the difference in A_{260} values reflected possible differences in how the tRNA were associated with the Arabidopsis tRNA nucleotidyltransferase. However, given where R64 is found in the primary sequence of the protein far from where tRNA are thought to interact, it is difficult to imagine what role position 64 could play in tRNA binding.

A previous study (Goring *et al*., 2013) showed no major changes in secondary structure among the native, E189F, R64W and R64WE189F proteins based on far UV-CD spectroscopy. However, given the overall large amount of α-helical character of tRNA nucleotidyltransferase proteins and the relatively small amount of β-sheet structure, *e.g*., Fig. 1-3, some small change in the single β-sheet may go unnoticed. In this context, it is interesting that R64 is found in one

strand of the single β-sheet contained in tRNA nucleotidyltransferase and that E189 is at the end of this β-sheet (Fig. 3-6). Perhaps altering these amino acids does not change the arrangement of the α-helices that make up most of the structure of the protein, but does affect the arrangement of the single β-sheet. Further study on the effects of these substitutions on the structure of the single β-sheet would be important. Fourier transformed infrared spectroscopy (FTIR) which is more sensitive to changes in β-sheet structure than is CD spectroscopy may provide more insight.

As seen previously for the native and E189F variant (Shan *et al*., 2008) there is no obvious large conformational change observed by far-UV CD spectroscopy and fluorescence experiments that can be defined as responsible for the increase in enzyme activity seen in the R64WE189F variant. To further explore how this variant results in the loss of the temperature-sensitive phenotype, enzyme activity was more carefully examined.

4.3 Enzymatic characterization

Previous characterization of the native and variant enzymes revealed an approximately 25-fold reduction in activity in the E189F variant (Shan *et al*., 2008) and an increase in activity in the R64WE189F variant to an intermediate value between those of the native and E189F enzymes (Goring *et al*., 2013). Based on these observations, it was proposed that the restoration of activity in the R64WE189F variant was sufficient to restore viability at the restrictive temperature and suppress the temperature-sensitive phenotype although the precise increase in activity was not determined (Goring *et al*., 2013). Here we set out to define precisely the scale of this increase in enzyme activity and to explore how changes in kinetic parameters resulted in the decrease in enzyme activity in the E189F variant and the restoration of this activity in the R64WE189F variant. It was hypothesized that a more detailed understanding of the activity of these variants would provide insight into the function of motifs A and C in the enzyme given that R64 maps to conserved motif A and E189 maps to conserved motif C (see Fig. 1-4).

Previous characterization of tRNA nucleotidyltransferases (Rether *et al*., 1974, Evans *et al.*, 1976, Deutscher., 1982, Reichert *et al.*, 2001) suggests that these enzymes follow classical Michaelis-Menten kinetics. With this in mind, apparent kinetic parameters for the native and

variant enzymes were determined using enzymatic assays. The assays contained a defined amount of radioactive tRNA template lacking its terminal adenosine residue, a mixture of yeast tRNA treated to remove its CCA sequence, CTP, ATP and the appropriate enzyme. Enzyme activity was defined by the addition of the specific adenosine residue to the radioactive substrate in the presence of increasing concentrations of unlabelled tRNA. The percent product was determined from a densitometric comparison of substrate and product levels at varying time points and substrate concentrations and these data were plotted to calculate initial rates such that a classical velocity versus substrate concentration graph could be generated.

In the first series of experiments, a variety of tRNA concentrations and times were used to generate product versus time plots. In each case the concentrations of ATP (1 mM) and CTP (0.4 mM) were held at approximately two fold their previously calculated K_M values, 560 μM and 180 μM, respectively (Chen *et al.*, 1990). Based on these data, substrate concentrations and time points were chosen to most effectively define initial velocities. With these values in hand, the initial velocities were plotted against the substrate concentrations for tRNA and GRAFIT software was used to determine apparent K_M and V_{max} values. As anticipated, the data showed hyperbolic profiles characteristic of enzymes that follow Michaelis-Menten kinetics (Fig. 3-5). The values determined represent apparent values because the reaction order is made pseudo-first order by using excess concentration of the other substrates and because there is no way of determining precisely what proportion of the added yeast tRNA contains all or some of their CCA sequence (although efforts were made to provide a uniform population of tRNA).

These apparent K_M and V_{max} values can provide us with information about the enzymatic reaction. For example, K_M serves as an indication of binding affinity. In contrast, V_{max} and the related value k_{cat} (turnover number) give an indication of the maximum reaction velocity. Taken together these simple parameters allow us to define some characteristics of the enzymes. Moreover, changes in these two parameters, as defined by the changes between the native and variant enzymes, may provide insight into the roles of the amino acids that are changed or the regions of the protein containing those amino acids.

4.3.1 K_M

In these experiments the concentrations of ATP and CTP were kept constant and at approximately twice their previously calculated K_M values, therefore, any change in apparent K_M value between different enzymes should reflect a change in tRNA binding to the various proteins. Given this, there is essentially no difference in tRNA binding between the native enzyme and any of the variants (Table 3-2). Even if one ignores the variability between experiments (standard error), the greatest difference in K_m is only 2-fold (between the native and R64W variant). The difference between the native and E189F is even less and it seems clear that these mutations do not affect tRNA binding to any great degree. This makes sense given that R64 and E189 are in motifs A and C respectively and tRNA binding is thought to take place all across the body and tail domains (Li *et al.*, 2002). Moreover, given that intracellular tRNA concentrations in yeast are in the range of 1-10 μM (Chu *et al*., 2011), the K_M values calculated here (1.1 – 2.2 μM) for tRNA are on the low end of this spectrum. It seems apparent that any slightly reduced tRNA binding to the E189F variant is not responsible for the observed temperature-sensitive phenotype. This is reinforced by the observation that the R64W variant shows no temperature-sensitive phenotype (Goring *et al*., 2013) but yet has an even greater apparent K_M (Table 3-2). Taken together these data strongly support what already is known about tRNA binding to tRNA nucleotidyltransferase and indicate that motifs A and C (as expected) are not involved in this process.

After the completion of this research, Matthew Leibovitch further characterized these variants and calculated K_M values for the nucleotide triphosphate substrates. For both ATP and CTP, he showed changes in K_M values of only about two to three fold, similar to the values obtained for tRNA binding as shown here. These data further support the idea that motif C is not involved directly with the binding of any of the substrates (Li *et al.*, 2002). More importantly, they show that the R64W change in motif A also does not alter nucleotide triphosphate binding. This further supports the proposed role of motif A in catalysis but not in nucleotide binding (Fig. 1-5, Li *et al*., 2002).

Given that the variant enzymes do not show any major changes in the binding of tRNA, ATP or CTP, this suggests that it is catalysis that is affected in these enzymes. Moreover, it is the decrease in catalytic activity in the E189F variant that leads to the temperature-sensitive phenotype and the restoration of this catalytic activity that leads to the loss of the temperature-sensitive phenotype in the R64WE189F suppressor.

4.3.2 k_{cat}

The parameter k_{cat} corresponds to the catalytic turnover rate of an enzyme. It describes the conversion of the ES (enzyme-substrate complex) to EP (free enzyme and product) and includes reaction chemistry and product release (Santos, 2010). As the enzyme variants showed no large variation in K_M for any substrate (ATP, CTP or tRNA) it seemed likely that the k_{cat} would define the differences between the various enzymes. This was indeed the case. The E189F variant had a k_{cat} value about 70-fold less than that of the native enzyme (Table 3-2). This decrease in k_{cat} correlates well with the 25-fold decrease in overall enzyme activity seen previously (Shan *et al*., 2008) and supports the hypothesis that the temperature-sensitive phenotype results from an enzyme with reduced activity (Goring *et al*., 2013) rather than reduced stability. Moreover, the viability of the R64WE189F suppressor strain at the restrictive temperature correlates well with an increase in turnover number of about six fold as compared to the E189F variant and a drop in activity of only about twelve fold (Table 3-2) as compared to the native enzyme. Similarly, that no phenotype was observed with the R64W variant reflects the small (1.3-fold) loss of activity in the R64W variant as compared to the native enzyme (Table 3-2). Taken together all of these data suggest that the mutation resulting in the E189F substitution drastically reduces enzyme activity to generate the temperature-sensitive phenotype while the suppressor mutation generating R64W restores this activity to a degree such that the cells can grow at the restrictive temperature.

In experiments carried out after this work had been completed, Matthew Leibovitch determined k_{cat} values when ATP or CTP substrate concentrations are altered and showed that these values are in good agreement with the values shown here. Whether tRNA, ATP or CTP concentrations are varied, there is a dramatic decrease in k_{cat} in the E189F variant (to approximately 1% of native) and a subsequent approximately 10-fold increase in k_{cat} in the

R64WE189F suppressor variant (Table 3-2). When all of these data are considered together they suggest that the E189F mutation alters the protein in some way such that catalysis is much less efficient. Moreover, the R64W mutation, which on its own does not decrease activity appreciably, actually restores activity about 10-fold in the context of the R64WE189F double mutant. Given that considerable research has gone into defining the interesting catalytic mechanism of tRNA nucleotidyltransferase (Yue *et al.*, 1998, Li *et al.*, 2002, Xiong *et al.*, 2004) and that neither of these residues has been shown to have a specific role in catalysis the question then remains as to how these amino acid substitutions could affect enzyme activity. To explore this question, molecular modelling was used.

4.4 Molecular modeling

A single amino acid substitution could affect enzyme activity by altering an amino acid required for catalytic activity. For example, Hanic-Joyce and Joyce (2002) showed that simply by converting in *Candida glabrata* the highly conserved aspartic acid residue (corresponding to D81 in the *Saccharomyces* enzyme) to alanine viability was lost. In another example, the *Bacillus stearothermophilus* tRNA nucleotidyltransferase was demonstrated to have its specificity altered by alteration of the residues E153, D154 and R157 defining the conserved EDxxR sequence of motif D (Cho *et al*., 2007). By reversing the hydrogen-bond polarity of two templating residues, the specificity was altered to UTP and GTP adding activities such that the enzyme would complete a UUG end (Cho *et al.*, 2007). Other amino acid substitutions may have a more indirect effect on enzyme activity. It has been demonstrated that deletion of a C-terminal region can confer CCA-adding activity to an A-adding enzyme (Tretbar *et al.*, 2011). Given that R64 and E189 are not highly conserved amino acids in tRNA nucleotidyltransferase (see Fig. 1-4) it seemed unlikely that they were directly involved in catalysis. Therefore, this suggested that these amino acids are more likely responsible for the spatial arrangement of other amino acids required for catalysis. To explore what changes may result from changes at positions 64 and 189 or both of these positions together molecular modelling was used.

As described in the results section SWISS-MODEL (Biasini *et al*., 2014) was used to model the native and variant tRNA nucleotidyltransferases. The existing crystal structure of the

Thermotoga maritima protein (PDB 3h38) was used as a template because it was the protein that showed the best native GMQE (0.48) and QMEAN4 (-11.43) values out of the elucidated crystal structures of tRNA nucleotidyltransferase. In addition, it also provided the most percent coverage for all variants at once. The other available templates: the *Homo sapiens* tRNA nucleotidyltransferase (PDB 1ou5), the *Bacillus stearothermophilus* tRNA nucleotidyltransferase (PDB 1miw) and the *Aquifex aeolicus* CC-adding (PDB 3WFO) and A-adding (PDB 1vfg) enzymes) gave GMQE and/or QMEAN4 scores only slightly lower (by about 1.5 points at most). Below the models will be used to develop a hypothesis as to why substrate binding is not dramatically affected in the variants but catalytic activity is.

Previous data suggested that the changes in the structure of the native, E189F, R64W and R64WE189F variants are quite small (Shan *et al*., 2008, Goring *et al*., 2013) and the models derived here are in good agreement with that (Fig. 3-7). There are no obvious dramatic changes in higher order structure in the models. To best exemplify any differences, one to one comparisons of the various proteins will be carried out here (Fig. 4-1 to Fig. 4-4). There are three questions that can be addressed here. 1) What change in the protein results in an almost 100-fold reduction in catalytic activity when E189 is changed to F? 2) Why does a subsequent R64W change in this defective protein restore activity about 10-fold? Finally, 3) if the R64W substitution increases activity of the E189F variant by 10-fold why does it not dramatically affect the activity of the native protein?

The active site of tRNA nucleotidyltransferase undergoes changes to motifs A-E during its shift of specificity from C-adding to A-adding activity. While motifs A (containing catalytic residues which coordinate the required metal ion), B (recognizing the ribose sugar), C (function unknown) and E (multiple roles in specificity and catalysis) move little during catalysis or ATP or CTP binding (Betat *et al.*, 2010), motif D changes its arrangement in space to hydrogen bond first with the incoming CTP and then the ATP in Watson-Crick-like base-pairs (Fig. 1-6) that exclude binding to UTP or GTP or even ATP or CTP at the wrong positions. Additionally, the 3'-end of the tRNA also must undergo a rotational and translational shift during the change from C addition to addition of the terminal A residue (Yamashita *et al*., 2014). Removing the flexible loop between motifs A and B abolishes (Fig. 1-7) the A-adding activity of tRNA nucleotidyltransferase suggesting that this region of the protein is required for the movement of

the tRNA within the active site and that its removal somehow restricts tRNA movement as that connecting region can act as a hinge/lever for conformational shifts (reviewed in Neuenfeldt *et al*., 2008). Knowing all of this, the effects of predicted changes in the structure of the tRNA nucleotidyltransferase that result from amino acid substitutions at position 64 and 189 can be linked to the changes in enzyme activity observed.

4.4.1 E189 change

If one initially examines the native enzyme (Fig. 3.6A) one sees that position 64 is part of a β-strand of the β-sheet that contains the catalytically important aspartic acid residues (Fig. 1-5). As for position E189, it is found in the final β-strand of this β-sheet and positioned at the interface of the neck and head domains. The model presented here differs slightly from one previously proposed by Shan *et al*. (2008) where E189 was hypothesized to be in a turn connecting this last β-sheet to the α-helix that follows it. Given that the present results implicate position E189 in an interaction with R64W and residues in catalytic domain located in motifs A-B that affect k_{cat} but with little to no effect on the residues of motif D and E which effect specificity and substrate recognition, I prefer the more recent model. From the models (Fig. 3-6A-D) it is apparent that residues adjacent to the β-sheet and those of the catalytic motifs (A-E) all point into the active site of the protein between the neck and head domains where the nucleotide triphosphates bind and catalysis takes place. If one compares the native and variant enzymes (Fig. 4-1 to 4-4) one can see that the catalytically important conserved residues D81 and D83 (in motif A), R171, R172 and D173 (in motif B) and, D216, D217 and R220 (in motif D) undergo slight changes in orientation due to movement of the backbone among all enzyme variants. As an enzyme's activity requires a precise arrangement of residues, the question then becomes, what changes in the arrangements of these amino acids can be correlated to changes in activity?

The conversion of the amino acid at position 189 from glutamate to phenylalanine, an amino acid of larger size (109Å^3 versus 135Å^3, Richards, 1974), leads to a loss of catalysis of 70 times the native turnover number (see Table 3-2). If one compares the models for the native and E189F variant (Fig. 4-1), one notes that largest movement at positions R64 and D83 (required in

motif B to coordinate the required metal ion, see Fig. 1-5) which move inward and E259 which moves outward. The changes are about 2Å while the rest of the side-chains show only slight changes in orientation. The simplest explanation for the drop in k_{cat} is that the required metal ion either is no longer bound by the conserved aspartic acid residues as D83 has moved in space relative to D81 or that if it is bound its orientation is changed such that it cannot act as a nucleophile to help catalyze the reaction. As these residues are not involved in substrate binding, the K_M increases very little as expected. Further, the residues of motif D seem to be affected the least by the introduction of a bulkier amino acid at position 189 (Fig. 4-1).

An alternate explanation may reflect more directly the movement of the tRNAs as happens during the course of catalysis. Within motif A, both residues R64 and D83 are displaced 2Å towards the center of the binding pocket in the E189F variant. As these side-chains protrude from the catalytically important β-sheet there would be less available space at the active site. By more tightly packing this region of the protein, there will be greater Van der Waal's constraints limiting the tRNA's ability to shift position for adenosine addition. If the tRNA is unable to shift position during the shift from C addition to A addition, then the rate of the reaction would be reduced.

To address these two possibilities one could initially increase the metal ion concentration in the reaction. If metal ion binding was decreased then increasing its concentration might ameliorate the reduction in catalytic rate. Subsequently one could use a min- or micro- tRNA which would reduce the size of the tRNA substrate to see what affect this had on catalysis in the native and E189F variant proteins. Also, it will be interesting to note whether the structure of the suppressor variant favors either of these hypotheses.

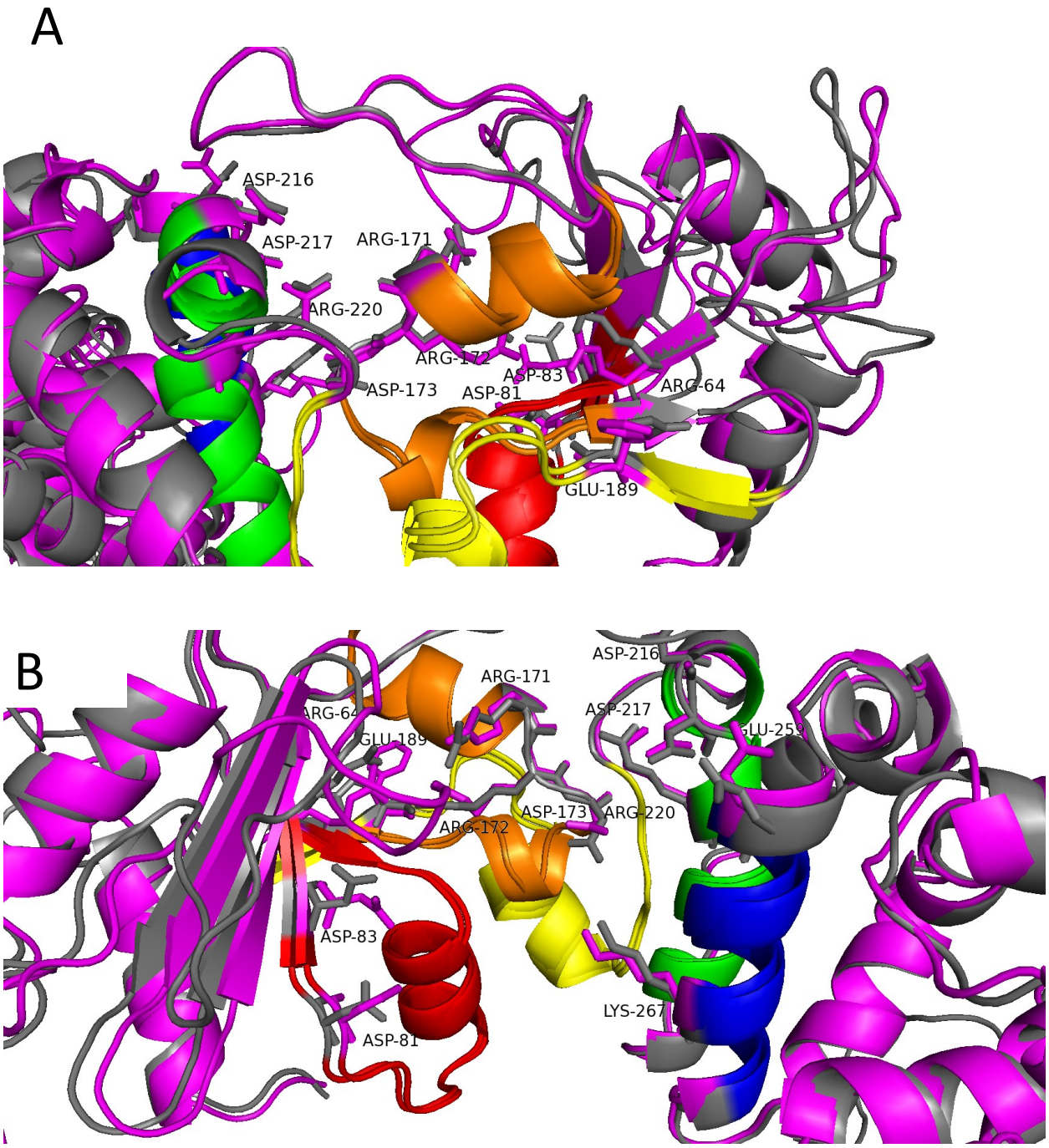

Figure 4-1. Model alignment of native and E189F. Native is colored in grey while E189F is colored in magenta.

4.4.2 R64W change

When in the native enzyme position 64 is changed to tryptophan (Fig. 4-2.), D83 does not change orientation appreciably (Fig. 4-2) even though the much larger tryptophan (163 $Å^3$) is present instead of the arginine (148 $Å^3$). In contrast, the position of E259 in motif E does change a lot (its oriented changes from inward to outward with respect to the active site) but it does not alter the k_{cat} of the enzyme (0.93 s^{-1}) which remains near native value (1.2 s^{-1}). Moreover, the position of E189 in the β-strand is altered. It appears that R64W does disturb the enzyme but, instead of altering the active site including a catalytically important residue of motif A, it alters the two hinge regions (motifs C and E) of the enzyme which seem to play only a limited role in catalysis. So, the R64W change on its own does not dramatically affect enzyme activity. How then does this change restore activity to the E189F variant? Is the outer surface of the protein becoming more flexible and extended?

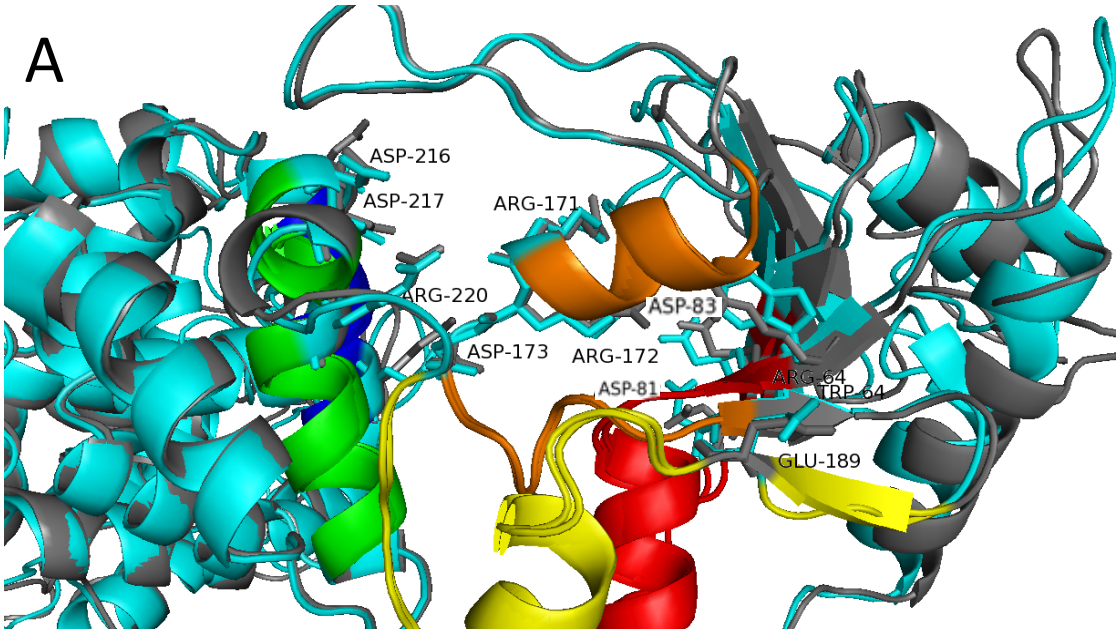

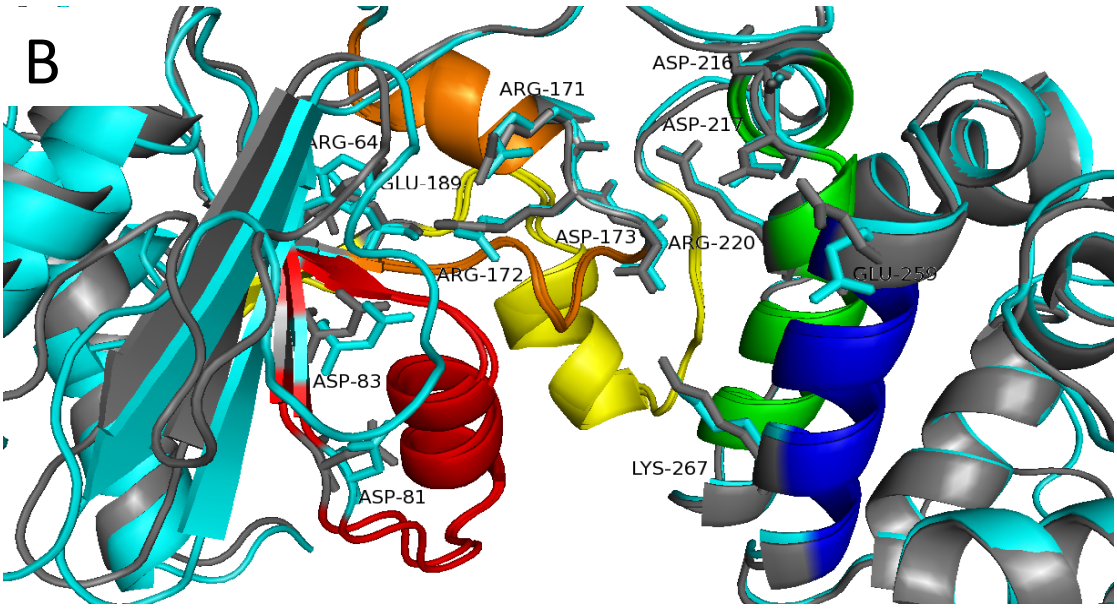

Figure 4-2. Model alignment of native and R64W. Native is colored in grey while R64W is colored in cyan.

4.4.3 R64WE189F change

When both tryptophan 64 and phenylalanine 189 are present the changes in position of amino acids (D83 and E259) observed in the E189F and R64W variants are reduced and closer to the native conformation(Fig. 4-4). In fact, the most dramatic change in position is seen for R171 of motif B's conserved RRD sequence which is important for deoxynucleotide recognition. While the measured k_{cat} (0.1 s^{-1}) is lower than that of the native or R64W (0.93 s^{-1}) variant it is sufficient to keep the cell alive. These data again support the role of the position of D83 in defining the catalytic rate of this enzyme.

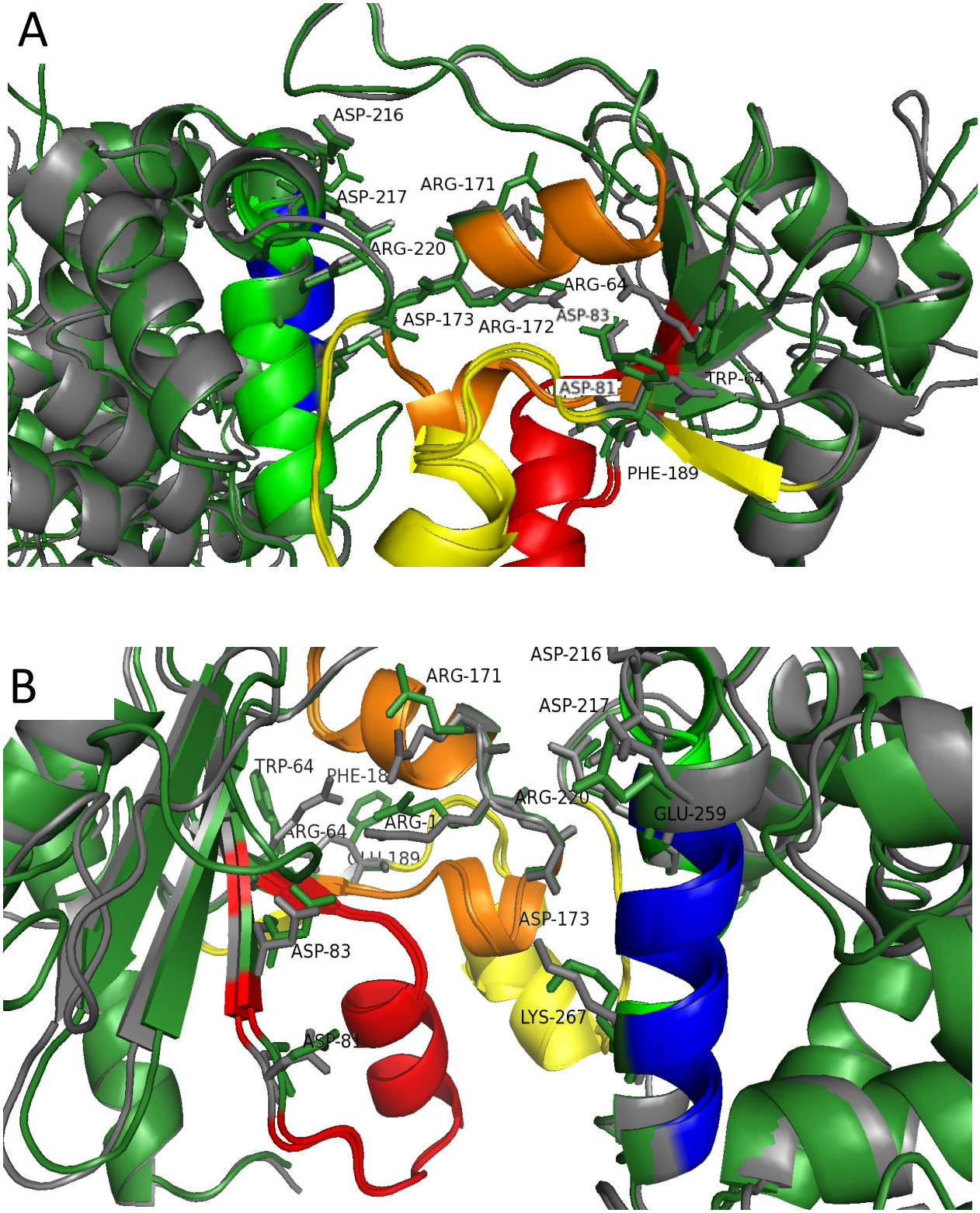

Figure 4-3. Model alignment of native and R64WE189F. Native is colored in grey while R64WE189F is colored in green.

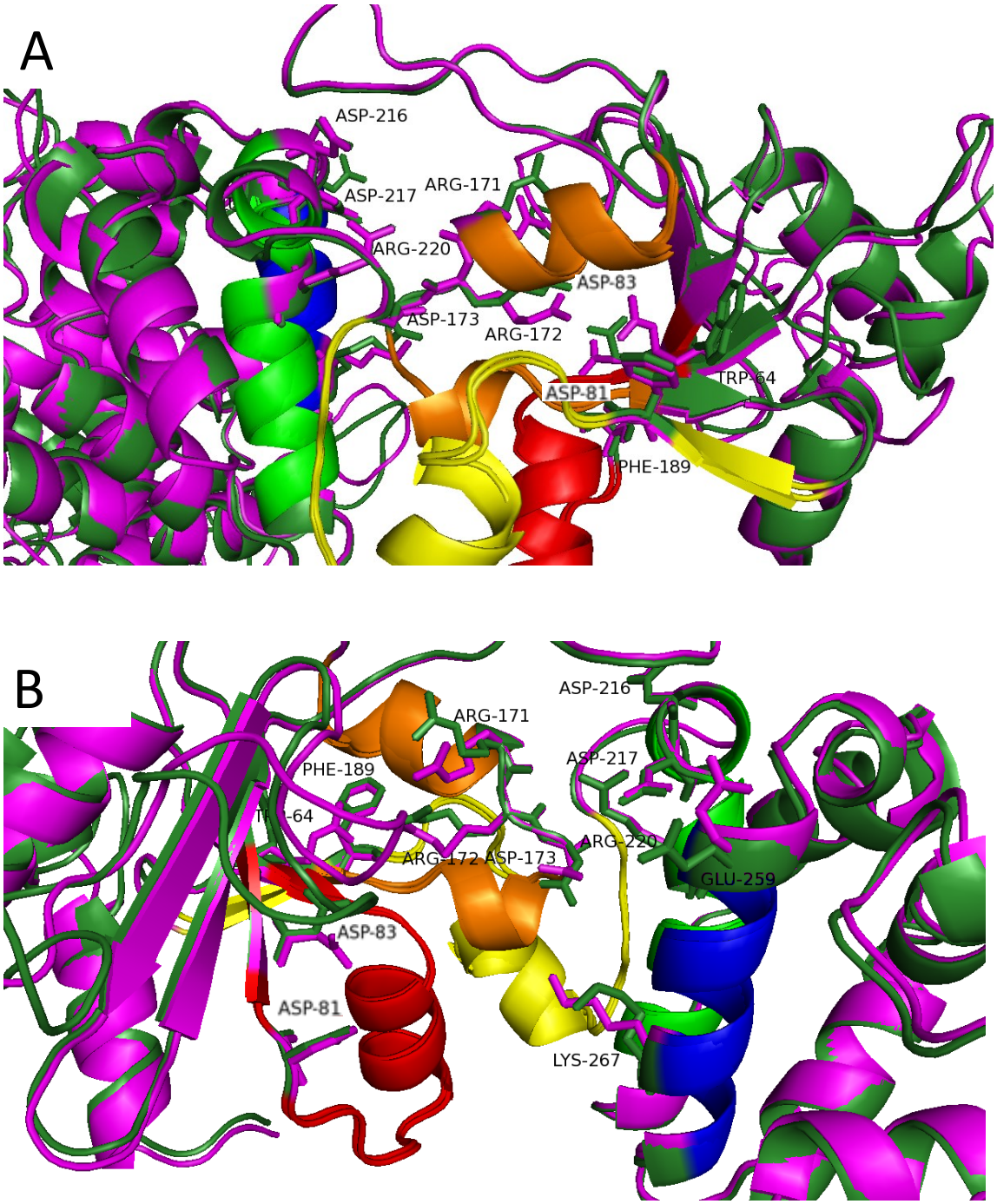

Figure 4-4. Model alignment of E189F and R64WE189F. E189F is colored in magenta while R64WE189F is colored in green.

4.5 In conclusion

This study of positions 64 and 189 of tRNA nucleotidyltransferase highlight motif C of its structure as an organizationally important region to the enzyme's active site. Moreover, motif E is also sensitive to the steric shifts along the catalytic beta-sheet.

BIBLIOGRAPHY

(1) Aebi, M.; Kirchner, G.; Chen, J. Y.; Vijayraghavan, U.; Jacobson, a; Martin, N. C.; Abelson, J. Isolation of a Temperature-Sensitive Mutant with an Altered tRNA Nucleotidyltransferase and Cloning of the Gene Encoding tRNA Nucleotidyltransferase in the Yeast *Saccharomyces cerevisiae*. *J. Biol. Chem.* **1990**, *265*, 16216–16220.

(2) Aravind, L.; Koonin, E.V. DNA Polymerase Beta-like Nucleotidyltransferase Superfamily: Identification of Three New Families, Classification and Evolution History. *Nucleic Acids Res.* **1999**, *27*, 1609-1618.

(3) Arthur, J. The Role of Arginine 244 in *Candida glabrata* tRNA Nucleotidyltransferase. Masters Thesis, Concordia University, Montreal, QC, 2009.

(4) Augustin, M. A.; Reichert, A. S.; Betat, H.; Huber, R.; Mörl, M.; Steegborn, C. Crystal Structure of the Human CCA-Adding Enzyme: Insights into Template-Independent Polymerization. *J. Mol. Biol.* **2003**, *328*, 985–994.

(5) Betat, H.; Rammelt, C.; Mörl, M. tRNA Nucleotidyltransferases: Ancient Catalysts with an Unusual Mechanism of Polymerization. *Cell. Mol. Life Sci.* **2010**, *67*, 1447–1463.

(6) Biasini, M.; Bienert, S.; Waterhouse, A.; Arnold, K.; Studer, G.; Schmidt, T.; Kiefer, F.; Cassarino, T.G.; Bertoni, M.; Bordoli, L.; Schwede, T. SWISS-MODEL: Modelling Protein Tertiary and Quaternary Structure Using Evolutionary Information. *Nucleic Acids Res.* **2014**, *42*, doi: 10.1093/nar/gku340.

(7) Chen, J. Y.; Kirchner, G.; Aebi, M.; Martin, N. C. Purification and Properties of Yeast ATP (CTP):tRNA Nucleotidyltransferase from Wild Type and Overproducing Cells. *J. Biol. Chem.* **1990**, *265*, 16221–16224.

(8) Chiemprasert, T.; Philipps, G.R. Hydrolysis of tRNA by Phosphodiesterase at Higher Temperatures. *Hoppe Seylers Z. Physiol. Chem.* **1976**, *11*, 1655-1658

(9) Cho, H. D.; Oyelere, A. K.; Strobel, S. a; Weiner, A. M. Use of Nucleotide Analogs by Class I and Class II CCA-Adding Enzymes (tRNA Nucleotidyltransferase): Deciphering the Basis for Nucleotide Selection. *RNA* **2003**, *9*, 970–981.

(10) Cho, H.D.; Verlinde, C. L. M.; Weiner, A. M. Reengineering CCA-adding Enzymes to Function as (U,G)- or dCdCdA-adding Enzymes or poly(C,A) and poly(U,G) Polymerases. *Proc. Natl. Acad. Sci. USA*. **2007**, *104*, 54-59.

(11) Chu, D.; Barnes, D.J.; von der Haar, T. The Role of tRNA and Ribosome Competition in Coupling the Expression of Different mRNAs in *Saccharomyces cerevisiae*. *Nucleic Acids Research*. **2011**, *39*, 6705-6714.

(12) Chu, H.Y. and Hopper, A. K. Genome-Wide Investigation of the Role of the tRNA Nuclear-Cytoplamsic Trafficking Pathway in Regulation of the Yeast *Saccharomyces cerevisiae* Transcriptome and Proteome. *Mol. Cell. Biol.* **2013**, *33*, 4241-4254.

(13) Czech, A.; Wende, S.; Mörl, M.; Pan, T.; Ignatova, Z. Reversible and Rapid Transfer-RNA Deactivation as a Mechanism of Translational Repression in Stress. *PLoS Genet*. **2013**, *9*, doi: 10.1371/journal.pgen.1003767

(14) Deng, X.Y.; Hanic-Joyce, P.J.; Joyce, P.B. Isolation and Nucleotide Sequence of a Gene Encoding tRNA nucleotidyltransferase from *Kluyveromyces lactis*. *Yeast*, **2000**, *16*, 945-952.

(15) Deutscher, M. Synthesis and Functions of the -C-C-A Terminus. *Progress in Nucleic Acids and Molecular Biology.* **1973**, *13*, 51-92.

(16) Deutscher, M.P. tRNA nucleotidyltransferase. *The Enzymes*. **1982**, *15,* 183-215.

(17) Evans, J.A.; Deutscher, M.P. Poly Amine Stimulation and Cation Requirements of Rabbit Liver Transfer RNA Nucleotidyl Transferase. *Journal of Biological Chemistry*. **1976**, *251*, 6646-6652.

(18) Feng, W.; Hopper, A.K. A Los1p-independent Pathway for Nuclear Export of Intronless tRNAs in *Saccharomyces cerevisiae*. *Proc. Natl. Acad. Sci. U.S.A.* **2002**, *99*, 5412-5417.

(19) Ghavidel, A.; Kislinger, T.; Pogoutse, O.; Sopko, R.; Jurisica, I.; Emili, A. Impaired tRNA nuclear export links DNA damage and cell-cycle checkpoint. *Cell*. **2007**, *131*, 915-926.

(20) Goring, M.E.; Leibovitch, M.; Gea-Mallorqui, E.; Karls, S.; Richard, F.; Hanic-Joyce, P.J.; Joyce, P.B. Characterization of Temperature-sensitivity and its Intragenic Suppression in *Saccharomyces cerevisiae* tRNA nucleotidyltransferase mutants. *Biochim. Biophys. Acta.* **2013**, *1834*, doi: 10.1016/j.bbapap

(21) Hanic-Joyce, P.J.; Joyce, P.B.M. Characterization of a Gene Encoding tRNA Nucleotidyltransferase from *Candida glabrata*. *Yeast*. **2002**, *19*, 1399-1411.

(22) Holm, L. and Sander, C. Mapping the Protein Universe. **1996**, *273*, 595-602.

(23) Larkin, M.A.; Blackshields, G.; Brown, N.P.; Chenna, R.; McGettigan, P.A.; McWilliams, H.; Valentin, F.; Wallace, I.M.; Wilm, A.; Lopez, R.; Thompson, J.D.; Gibson, T.J.; Higgins, D.G. Clustal W and Clustal X version 2.0. *Bioinformatics*. **2007,** *23*, 2947-2948.

(24) Leibovitch, M.; Bublak, D.; Hanic-Joyce, P.J.; Tillmann, B.; Flinner, N.; Amsel, D.; Scharf, K.D.; Mirus, O.; Joyce, P.B.M.; Schleiff, E. The Folding Capacity of the Mature Domain of the Dual-Targeted Plant tRNA nucleotidyltransferase Influences Organelle Selection. *Biochemical Journal*. **2013**, *453*, 401-412.

(25) Li, F.; Xiong, Y.; Cho, H.D.; Tomita, K.; Weiner, A.M.; Steitz, T.A. Crystal Structures of the *Bacillus stearothermophilus* CCA-adding Enzyme and Its Complexes with ATP or CTP. *Cell*. **2002**, *111*, 815-824.

(26) Lizano, E.; Scheibe, M.; Rammelt, C.; Betat, H.; Mörl, M. A Comparative Analysis of CCA-adding Enzymes from Human and *E. coli*: Differences in CCA Addition and tRNA 3'-end Repair. *Biochimie*. **2008**, *90*, 762-772.

(27) Murthi, A.; Shaheen, H.H.; Huang, H.Y.; Preston, M.A.; Lai, T.P., Phizicky, E.M.; Hopper, A.K. Regulation of tRNA Bidirectional Nuclear-Cytoplasmic Trafficking in *Saccharomyces cerevisiae*. *Mol. Biol. Cell.* **2010**, *21*, 639-649

(28) Nagaike, T.; Suzuki, T.; Tomari, Y.; Takemoto-Hori, C.; Negayama, F.; Watanabe, K.; Ueda, T. Identification and Characterization of Mammalian Mitochondrial tRNA Nucleotidyltransferases. *J. Biol. Chem.* **2001**, *26*, 40041-40049.

(29) Neuenfeldt, A.; Just, A.; Betat, H.; Mörl, M. Evolution of tRNA Nucleotidyltransferases: A Small Deletion Generated CC-adding Enzymes. *Proc. Natl. Acad. Sci. U.S.A.* **2008**, *105*, doi: 10.1073/pnas.0801971105

(30) Oh, B. K.; Pace, N. R. Interaction of the 3'-End of tRNA with Ribonuclease P RNA. *Nucleic Acids Res.* **1994**, *22*, 4087–4094.

(31) Peltz, S.W.; Donahue, J.L.; Jacobson, A. A Mutation in the Transfer-RNA Nucleotidyltransferase Gene Promotes Stabilization of Messenger-RNAs in *Saccharomyces cerevisiae*. *Molecular and Cellular Biology*. **1992**, *12*, 5778-5784.

(32) Reichert, A.S.; Thurlow, D.L.; Mörl, M. A Eubacterial Origin for the Human tRNA Nucleotidyltransferase. *Biol Chem*. **2001**, *382*, 1431-1438

(33) Rether, B.; Bonnet, J.; Ebel, J.P. Studies on tRNA Nucleotidyltransferase from Baker's Yeast. **1974**, *50*, 281-288.

(34) Richards, F. M. The Interpretation of Protein Structures: Total Volume, Group Volume Distributions and Packing Density. *Journal of Molecular Biology*. **1974**, *82*, 1-14.

(35) Sambrook, J., Maniatis, T., Fritch, E,F. (1989). Molecular Cloning 2nd Ed., Cold Spring Harbor Laboratory Press.

(36) Santos, M. N. A General Treatment of Henri-Michaelis-Menten Enzyme Kinetics: Exact Series Solution and Approximate Analytical Solutions. *MATCH Commun. Mat. Comput. Chem.*, **2010**, *63*, 283-318.

(37) Sarin, P.S.; Zamenick, P.C. On The Stability of Aminoacyl-S-RNA to Nucleophilic Catalysis. *Biochim. Biophys. Acta.* **1964**, *91*, 653-655.

(38) Schmidt, S.; Sabetti, A.; Hanic-Joyce, P.J.; Gu, J.; Schleiff, E.; Joyce, P.B. Dual Targeting of the tRNA Nucleotidyltransferase in Plants: Not Just the Signal. *J. Exp. Bot.* **2007**, *58*,
(39) Shan, X.; Russell, T. A.; Paul, S. M.; Kushner, D. B.; Joyce, P. B. M. Characterization of a Temperature-Sensitive Mutation That Impairs the Function of Yeast tRNA Nucleotidyltransferase. *Yeast* **2008**, *25*, 219–233.

(40) Shanmugam, K.; Hanic-Joyce, P.J.; Joyce, P.B. Purification and Characterization of a tRNA Nucleotidyltransferase from *Lupinus albus* and Functional Complementation of a Yeast Mutation by Corresponding cDNA. *Plant. Mol. Biol.* **1996**, *30*, 281-295.

(41) Sprinzl, M.; Cramer, F. The -C-C-A end of tRNA and its role in protein biosynthesis. *Progress Nucleic Acid Research and Molecular Biology*. **1979**, *22*, 1-69.

(42) Toh, Y.; Takeshita, D.; Numata, T.; Fukai, S.; Nureki, O.; Tomita, K. Mechanism for the Definition of Elongation and Termination by the Class II CCA-adding Enzyme. *EMBO J.* **2009**, *28*, doi: 10.1038/emboj.2009.260

(43) Tomita, K.; Yamashita, S. Molecular Mechanisms of Template-independent RNA Polymerization by tRNA Nucleotidyltransferases. *Front Genet*. **2014**, *5*, doi: 10.3389/fgene.2014.00036

(44) Tomita, K.; Fukai, S.; Ishitani, R. Ueda, T.; Takeurchi, N.; Vassylyev, D.G.; Nureki, O. Structural Basis for Template-Independent RNA Polymerization. **2004**, *430*, 700-704.

(45) Tretbar, S.; Neuenfeldt, A.; Betat, H. Morl, M. An Inhibitory C-terminal Region Dictates the Specificity of A-adding Enzymes. *Proc. Natl. Acad. Sci. U.S.A*. **2011**, *108*, 21040-21045.

(46) Vortler, S.; Moerl, M. tRNA-nucleotidyltransferases: Highly Unusual RNA Polymerases with Vital Functions. *FEBS LETTERS*, **2010**, *584*, 297-302.

(47) Whitney, M.L.; Hurto, R.L.; Shaheen, H.H.; Hopper, A.K. Rapid and Reversible Nuclear Accumulation of Cytoplasmic tRNA in Response to Nutrient Availability. *Mol. Biol. Cell.* **2007**, *18*, 2678-2686.

(48) Wong C, Sridhara S, Bardwell JC, Jakob U. Heating greatly speeds Coomassie blue staining and destaining. *Biotechniques*. **2000**, *28*, 426-8, 430, 432.

(49) Wilusz, J.E.; Whipple, J.M.; Phizicky, E.M.; Sharp, P.A. tRNAs Marked With CCACCA Are Targeted for Degradation. *Science*. **2011**, *334*, 817-821.

(50) Xiong, Y.; Steitz, T. a. Mechanism of Transfer RNA Maturation by CCA-Adding Enzyme without Using an Oligonucleotide Template. *Nature.* **2004**, *430*, 640–645.

(51) Yamada, M.; Ohki, M; Ishikura, H. The Nucleotide Sequence of Bacillus-Subtilis Transfer-RNA Genes. *Nucleic Acids Research.***1983**, *11*, 3037-3045.

(52) Yamashita, S.; Takeshita, D.; Tomita, K. Translocation and Rotation of tRNA during Template-Independent RNA Polymerization by tRNA Nucleotidyltransferase. *Structure*. **2014**, *22*, 315-325.

(53) Yue, D.; Maizels, N.; Weiner, A.M. CCA-adding Enzymes and Poly(A) Polymerases Are All Members of the Same Nucleotidyltransferase Superfamily: Characterization of the CCA-adding Enzyme from the Archaeal Hyperthermophile *Sulfolobus shibitae*. *RNA*. **1996**, *2*, 895-908.

(54) Yue, D.; Weiner, A.M.; Maizels, N. The CCA-adding Enzyme Has a Single Active Site. *Journal o Biological Chemistry*. **1998**, *273*, 29693-29700.

(55) Zasloff, M.; Rosenberg, M.; Santos, T. Impaired Nuclear Transport of a Human Variant Transfer RNAIMET. *Nature*. **1982**, *300*, 81-84.

(56) Zasloff, M. tRNA Transport From The Nucleus In A Eukaryotic Cell: Carrier-mediated Translocation Process. *Proc. Natl. Sci.* **1983**, *80*, 6435-40.

(57) Zhu, L.; Deutscher, M.P. tRNA Nucleotidyltransferase Is Not Essential for *Escherichia coli* Viability. *EMBO J*. **1987**, *6*, 2473-2477.

6. Appendix I - E189K and E189RR64E

Converting E189 to K generates a model where the D81 is the most affected amino acid. The effect appears similar from a model perspective.

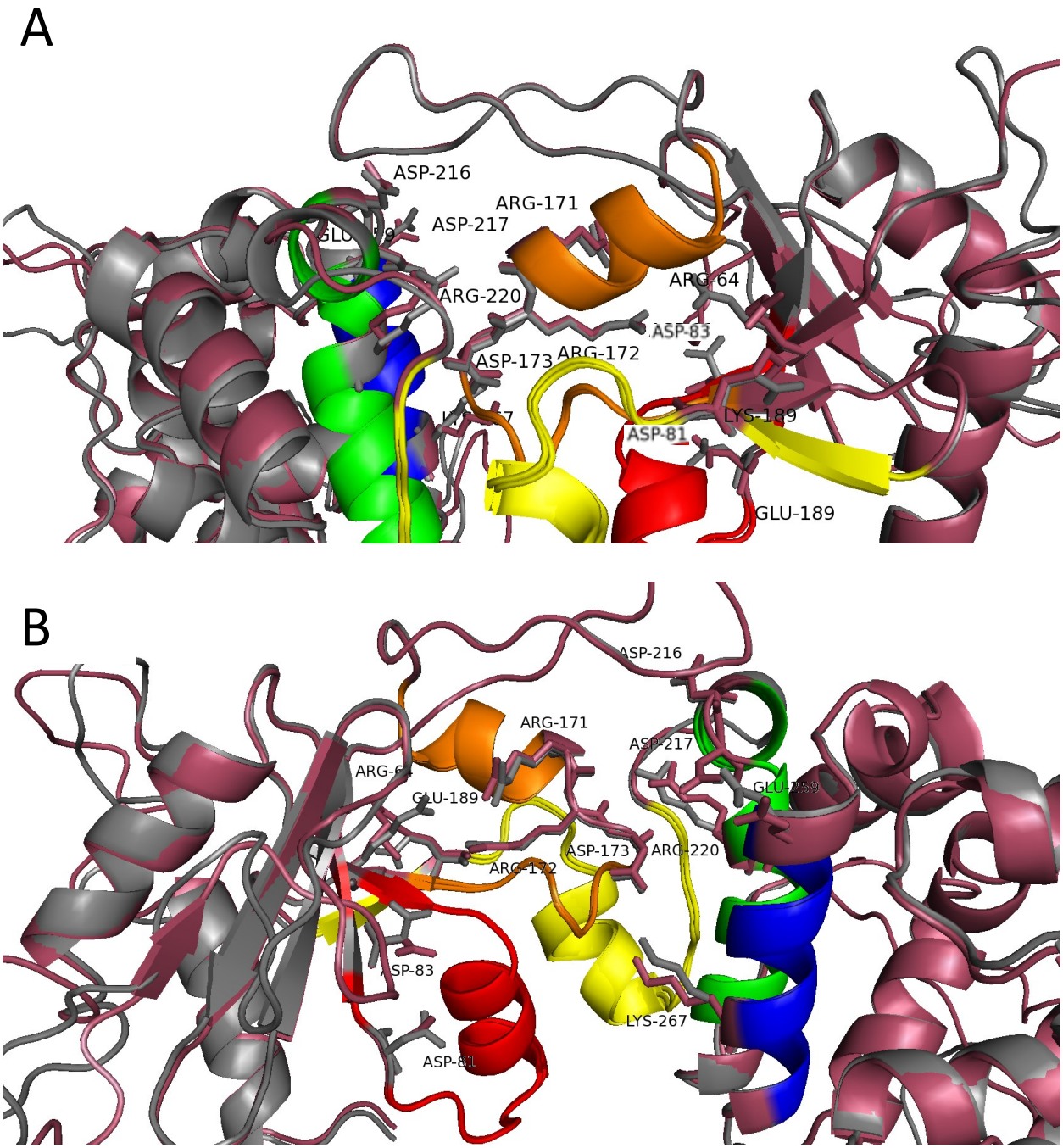

Figure 6-1. Model alignment of native and E189K. Native is grey while E189K is rose.

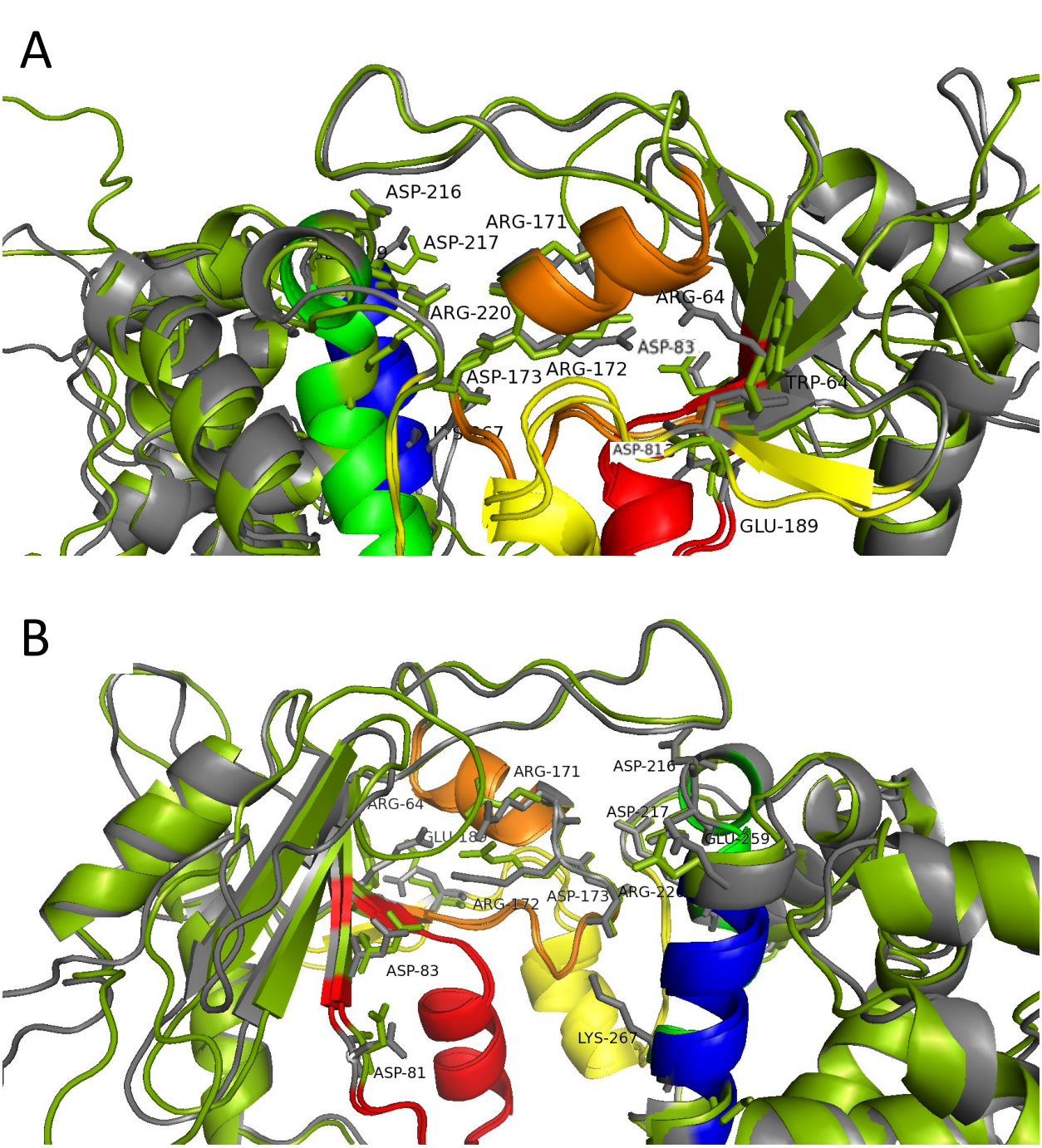

Figure 6-2. Model alignment of native and R64WE189K. Native is grey while R64WE189K is green.

Furthermore, in the molecular models built from E189RR64E, the β-strand is no longer present at position E189 owing to the arginine's high flexibility hindering stability of motif C. Conversion of the arginine at position 64 to a glutamate does not affect any of the residues much.

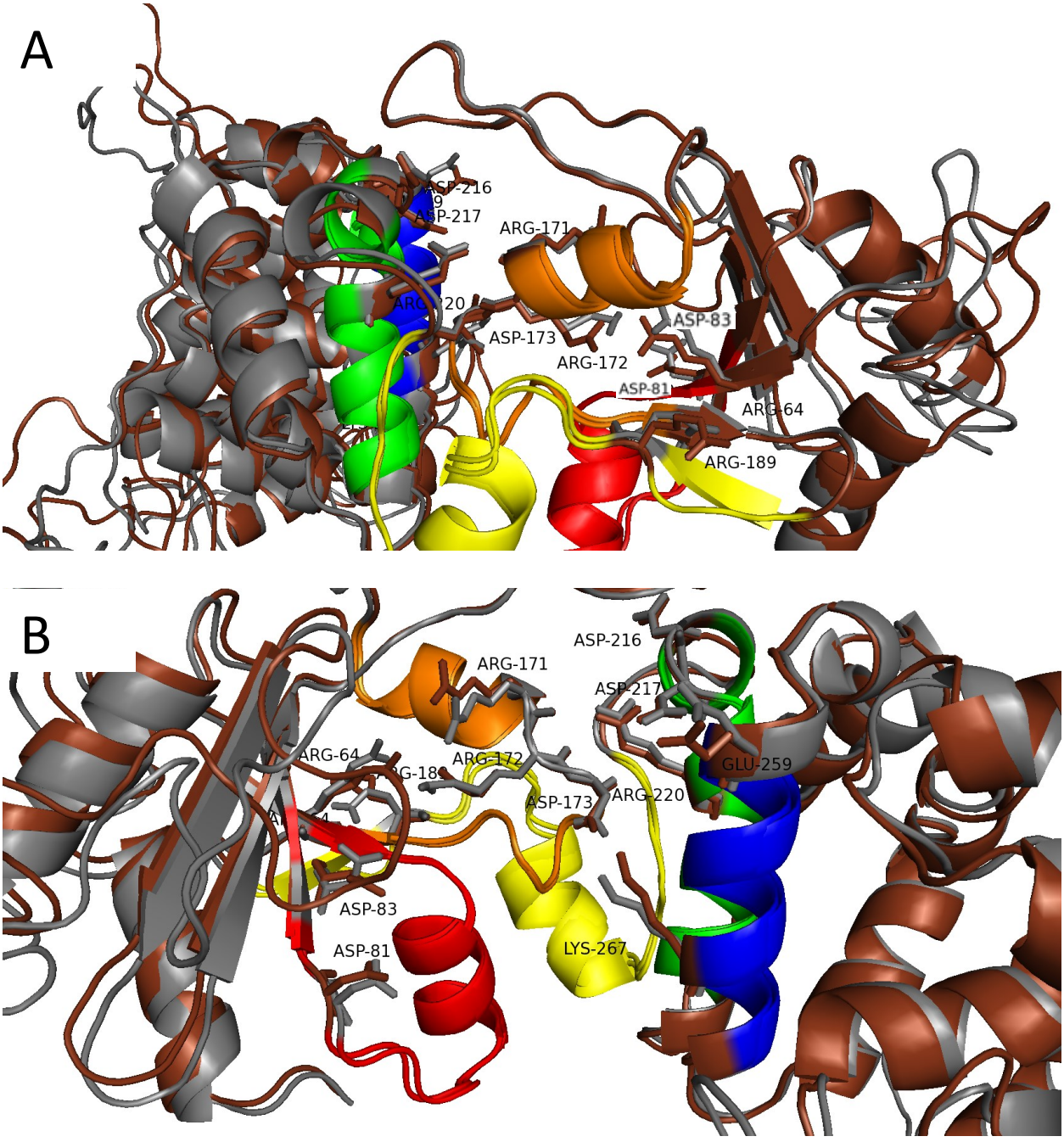

Figure 6-3. Model alignment of native and E189R. Native is grey and E189R is brown.

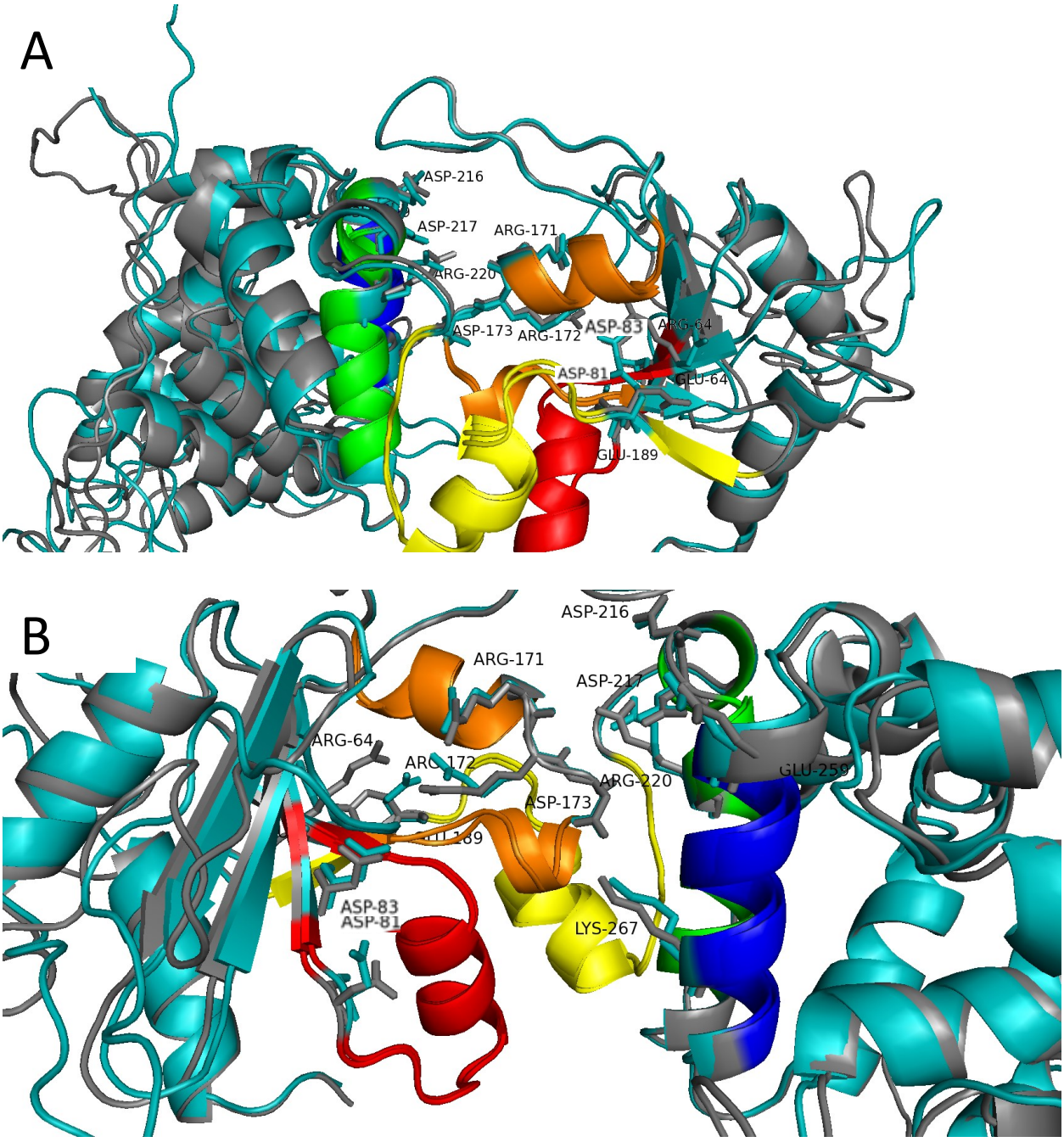

Figure 6-4. Model alignment of native and R64E. Native is grey and R64E is cyan.

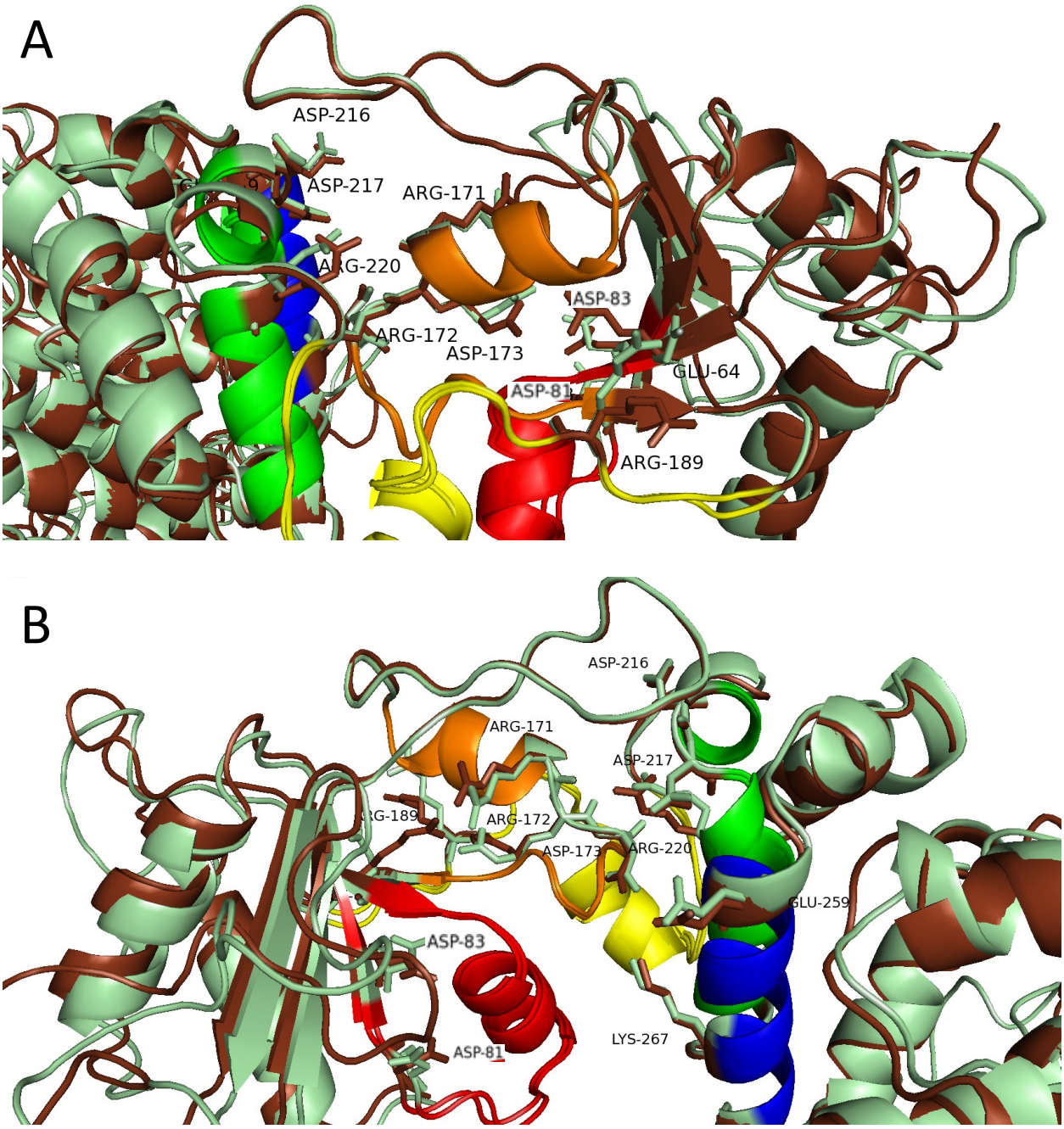

Figure 6-5. Model alignment of E189R and R64EE189R. E189R is brown while R64EE189R is green.